nature reviews physics
https://doi.org/10.1038/s42254-024-00703-6

Review article

Check for updates

Anomalies in particle physics and their implications for physics beyond the standard model

Andreas Crivellin [1,2] ✉ & Bruce Mellado [3,4] ✉

Abstract

The standard model (SM) of particle physics is the mathematical description of the fundamental constituents and interactions of matter. Its last missing particle, the Higgs boson, was observed in 2012. However, there are several phenomena that the SM cannot account for (such as dark-matter particles, or non-vanishing neutrino masses), neither does it describe gravity. There must be more to discover, to extend the SM into a full description of nature. Here we review the hints of new physics, called anomalies, that are seen for various interactions as discrepancies between standard-model predictions and experimental measurements. We consider both direct high-energy searches for new particles at the Large Hadron Collider at CERN and indirect low-energy precision experiments. These anomalies span an energy scale of more than four orders of magnitude: from the mass of the proton, to the electroweak scale (approximately the mass of the Higgs boson), to the teraelectronvolt scale, which is the highest scale directly accessible at the Large Hadron Collider. We discuss the experimental and theoretical status of various anomalies and summarize possible explanations in terms of new particles and new interactions as well as discovery prospects. We suggest, in particular, that new additional Higgs bosons and so-called leptoquarks are promising candidates for extending the standard model.

Sections

[1]Physik-Institut, Universität Zürich, Zürich, Switzerland. [2]Paul Scherrer Institut, Villigen PSI, Switzerland. [3]School of Physics and Institute for Collider Particle Physics, University of the Witwatersrand, Johannesburg, Wits, South Africa. [4]iThemba LABS, National Research Foundation, Somerset West, South Africa. ✉e-mail: andreas.crivellin@psi.ch; bmellado@mail.cern.ch

Key points

- The standard model (SM) of particle physics describes the fundamental constituents of matter and their interactions and was completed with the discovery of the Higgs particle at the Large Hadron Collider (LHC) at CERN in 2012.
- The SM cannot account for the existence of dark matter or for non-vanishing neutrino masses and must therefore be extended, but there is a plethora of viable options for this extension.
- In experiments, several interesting deviations from the standard-model predictions have been found. These anomalies appear both in high-energy searches at the LHC and in low-energy precision observables: ranging from precision measurements of properties of the muon, to hints for new scalar bosons at the electroweak scale, to the existence of heavy teraelectronvolt-scale resonances.
- The anomalies can be explained by supplementing the SM with new particles and new interactions — in particular, additional Higgs bosons, new fermions and new strongly interacting particles.
- Data accumulating from the third run of the LHC could establish the existence of some of these new particles, if one or more of the anomalies are indeed driven by new physics. The high-luminosity upgrade of the LHC, future linear or circular colliders and new precision experiments will be needed for a comprehensive study of the properties of particles.

Introduction

The standard model (SM) of particle physics is the currently accepted mathematical description of the fundamental constituents of matter and their interactions (excluding gravity). With the discovery of the famous Higgs particle[1,2] at CERN's Large Hadron Collider (LHC) in 2012[3,4], the SM is now complete (Box 1).

However, the SM cannot be the ultimate fundamental theory of nature. In addition to many theoretical arguments for the existence of physics 'beyond the SM' (BSM), the SM itself has several shortcomings. It cannot, for example, account for observations of dark matter at cosmological scales, as it does not contain a weakly interacting particle with the correct relic abundance. Neither can it account for the non-vanishing neutrino masses required to explain neutrino oscillations: SM neutrinos, which are left-handed, are necessarily massless owing to the absence of a right-handed partner (neutrino masses can be induced in a minimal way by adding right-handed neutrinos, but we consider that to be BSM physics). Unfortunately, no right-handed neutrinos have been observed; experiments aiming to directly detect dark matter have not seen any signal[5]. Thus, in the absence of such experimental results, there remain many options for how the SM can be extended to account for dark matter and neutrino masses, spanning a very large mass range from several kiloelectronvolts to the scale of Grand Unification at around 10^{15} GeV (Box 2).

The SM has been extensively tested[6] and the search for new physics has continued over the past decade, both in high-energy searches (mainly at the LHC) and in precision experiments that probe accurately the properties of known particles. High-energy experiments are trying to produce new particles directly in the form of resonances (peaks in kinematic distributions) and thus are able to measure particle mass directly. Precision experiments look for the effects of new particles seen via quantum fluctuations; these experiments can determine the ratio of coupling squared to the square of the mass scale, but not the particle mass itself. However, such indirect searches for new physics are able to test higher energy scales than those that can be accessed directly at the LHC (which is limited to a bit less than half the centre-of-mass energy, ~6 TeV).

In fact, an increasing number of hints for new physics have been reported in the form of deviations of experimental measurements from SM predictions and are called 'anomalies'. They span a huge energy range and include precision measurements such as the anomalous magnetic moment of the muon, semi-leptonic B meson decays and the measurement of the W boson mass; also direct LHC searches, and even non-resonant searches for particles too heavy to be produced directly at the LHC.

Probability theory and statistics tell us that one cannot expect that all these anomalies will be confirmed in the future, but it is also unlikely that all of them are just statistical flukes or due to experimental errors. Therefore, it is important to assess the strengths and weaknesses of these anomalies and to consider which extensions of the SM they suggest, to be able to predict which signals to seek for future verification or falsification. In this article, we will review the status of these anomalies, give an overview of how they can be explained by BSM physics and provide an outlook on future implications.

What constitutes an anomaly

An anomaly is generally defined as a deviation from the common rule. In particle physics, it entails a discrepancy between the experimental data and the corresponding SM prediction. Many anomalies presently exist, so objective selection criteria are essential to choose which should be considered for further scrutiny.

Here we employ the following criteria:

- The combined global statistical significance should be at least three standard deviations (3σ), after the application of trial factors and look-elsewhere effects. As such, we allow for the combination of several channels or measurements if they are related to the same effective interactions or simplified model parameters.
- The experimental signature should include more than a single channel (or observable) or be measured (probably with lower significance) by more than one independent experiment.
- The deviation should be described by a theoretically robust model that does not contradict the wealth of existing constraints from other measurements in particle physics.

In general, the discovery threshold in particle physics is taken to be 5σ. This means that the probability of a statistical fluctuation is about one in 3.5 million. However, estimating the systematic uncertainty is often very difficult and the probability of human error is not included in the statistical significance. Therefore, this definition is only applied if the situation is 'clear' — by which we mean that the measurement is to some extent explainable by a well-defined model. This was the case, for example, for the top quark and the Higgs boson, as the SM required their existence. However, for unexpected measurements, one usually requires very high standards concerning the systematic uncertainties (both on the experimental and the theoretical side) and independent confirmation by another experiment or channel.

The analysis of an anomaly proceeds differently for direct versus indirect searches. For low-energy precision observables, it can often

Box 1

The standard model

The particle content of the standard model comprises quarks, leptons, gauge bosons and the Higgs particle (see the figure).

Matter consists of quarks and leptons, both of which are fermions (spin-1/2 particles). A proton contains two up-quarks (u with electric charge +2/3) and one down-quark (d with charge −1/3); a neutron consists of one up-quark and two down-quarks. Electrons (e) constitute the atomic shell. Together with the nearly massless and very weakly interacting neutrinos (ν), they form the class called leptons. All fermions appear in three copies, called generations or flavours, that differ in mass (more precisely, all differences between the generations of fermions are induced by the mass terms originating from their couplings to the Higgs particle). The electron is accompanied by its heavy cousins the muon (μ) and the even heavier tau (τ). The more-massive versions of the up-quark are called charm (c) and top (t); strange (s) and bottom quark (b) are the heavier copies of the down-quark. The masses of the charged fermions range from ~0.0005 GeV for the electron to ~174 GeV for the top. Only first-generation fermions are stable, the heavier generations are short-lived and decay to lighter flavours.

The forces between the fermions are mediated by gauge interactions based on local symmetries. The gauge group of the SM is $SU(3)_c \times SU(2)_L \times U(1)_Y$, which corresponds to rotations in 3D, 2D and 1D (external) complex spaces. Owing to the wave-particle duality of quantum mechanics, these interactions result in force particles — the gauge bosons, which are spin-1 particles. The electromagnetic force is mediated by the photon (γ). The weak force (corresponding to the $SU(2)_L$ factor) is mediated by two charged W and one neutral Z gauge bosons (strictly, the photon and the Z boson are linear combinations of the $U(1)_Y$ boson and the neutral component of $SU(2)_L$). The strong force ($SU(3)_c$) is carried by eight gluons (g). Neutrinos only feel the weak force, but the charged leptons (electron, muon and tau) have electromagnetic as well as weak interactions, and quarks in addition have colour charges and interact with gluons under the strong force. Importantly, all flavour violation (that is, non-conservation of flavour) in the SM is induced by the couplings of the W boson to up-type and down-type quarks via the Cabibbo–Kobayashi–Maskawa matrix, a 3×3 matrix whose elements account for the corresponding coupling strength.

Finally, there is the Higgs particle — the first and (so far) only fundamental scalar particle (spin 0). The field from which the Higgs boson originates spontaneously breaks $SU(2)_L \times U(1)_Y$ to the electromagnetic gauge group $U(1)_{EM}$ with the massless photon. At the same time, it gives masses to the W (~80 GeV) and Z bosons (~90 GeV) as well as to all (fundamental) fermions and the Higgs boson itself (~125 GeV).

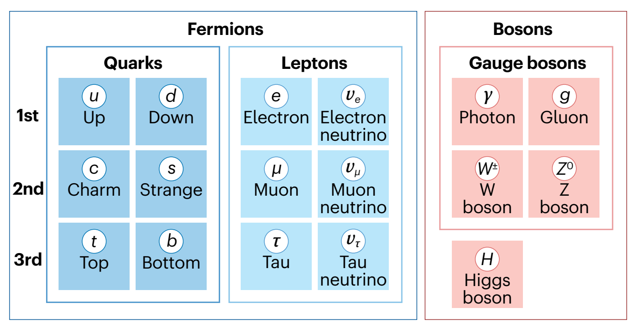

be assumed that the scale of new physics is higher than the energy scale of the experiment. The consistency and significance of several measurements can then be evaluated using an effective field theory (EFT) approach. In this setup, the interactions parameterizing the new-physics effects are required to respect fundamental symmetries such as charge conservation and Lorentz invariance. Then, in a later step, it can be assessed which model of new physics gives rise to the desired effective interactions, while at the same time avoiding the constraints of other observables that are not directly connected within the effective setup (but only arise once the new particle content is known).

For direct searches, aiming at the production of new particles, an EFT approach is not possible: the new particles are dynamic degrees of freedom and cannot be integrated out to obtain effective interactions. However, in many cases, it is possible to study simplified models, in which only a single new field with the relevant couplings to the SM is added. Nonetheless, different measurements can still be combined if there is consistency in the suggested masses of the new particles. Furthermore, by assuming specific coupling structures – for example, that a new Higgs is SM-like – the number of free parameters can be reduced.

Importantly, if any anomaly in direct or indirect searches were confirmed beyond reasonable doubt, this would inevitably imply the breakdown of the SM and require its extension with new particles and new interactions (Fig. 1).

Key anomalies in particle physics

We now present what we consider to be the key anomalies in present experimental data and discuss how each could be explained by new physics. The anomalies are listed in the order of increasing energy scale, as represented in Fig. 2. The extensions of the SM to which they point are shown in Fig. 3.

Anomalous magnetic moment of the muon

For any fundamental fermion, the Dirac equation predicts that the ratio of its magnetic moment to its angular momentum – the gyromagnetic ratio, or g-factor – is exactly 2. However, the famous prediction of quantum electrodynamics (the quantum field theory of electromagnetism), made by Julian Schwinger[7] (Fig. 1a), was a positive shift owing to quantum fluctuations of $a_\ell = (g-2)_\ell/2$, for a lepton ℓ (electron, muon or tau); for the electron, simply, $a_e = \alpha/(2\pi)$, in which α is the fine structure constant. This is known as the Schwinger term of the anomalous magnetic moment.

Although the prediction for the electron has been calculated very precisely and matches reasonably well with the experiment, in the case of the anomalous magnetic moment of the muon, a_μ, the combined value of the 2006 result of the E821 experiment[8] at Brookhaven National Laboratory, USA, and the recent $g-2$ experiment[9,10] at Fermilab, USA, deviates from the SM prediction made by the $g-2$ theory initiative[11] by 5.1σ. However, this SM prediction is plagued with sizable hadronic effects (unlike in the case of the electron), and measurements of electron–positron scattering that produce hadrons[12–14] are needed to extract these effects. The significance of the deviation is also challenged by the so-called lattice simulations of quantum chromodynamics (QCD, the quantum field theory describing the strong interactions)[15] and the latest measurement of $e^+e^- \to$ hadrons by the CMD 3 collaboration[16], which would render the SM prediction closer to the measurement[17]. A positive shift in a_μ of the order of 10^{-9} is certainly preferred but, owing to the tensions among the different SM predictions, a reliable estimate of the significance of the deviation is not possible at the moment.

The anomalous magnetic moment of the electron is measured and predicted much more precisely than a_μ, hence the resulting bounds on new physics are stringent[18–20]. Therefore, the effect of new physics on a_e must be smaller than that on a_μ and would thus violate lepton flavour universality[21] (see ref. 22 for an overview of new physics in a_μ). Furthermore, the new physics must be quite light: for example, a viable option[23,24] is a light Z' boson coupling to muons but not to electrons, with a mass below the muon threshold (~0.2 GeV) to avoid limits from $e^+e^- \to 4\mu$ from BaBar[25] at SLAC National Accelerator Laboratory, USA, and Belle[26] at KEK, Japan. Alternatively, if the new physics is heavy (at the teraelectronvolt scale), it must possess an enhancement factor. This can be provided via the mechanism of chiral enhancement, meaning that the chirality flip does not originate from the small muon Yukawa coupling (as it does for the SM contribution to a_μ) but from a larger coupling of other particles to the SM Higgs. In the minimal supersymmetric SM, this factor is tanβ, the ratio of the

Box 2

Possible extensions of the standard model

To build a consistent renormalizable extension of the standard model (SM), only scalars bosons (spin 0), fermions (spin 1/2) and vectors bosons (spin 1) are at our disposal — provided that, in the latter case, a Higgs-like mechanism of spontaneous symmetry-breaking exists to generate their masses. We focus on the following SM extensions.

Leptoquarks

- Scalar or vector bosons that carry colour and couple quarks directly to leptons[292,293]. These particles were first proposed in the context of quark–lepton unification at high energies, namely, the Pati–Salam model[294] and grand unified theories (GUTs)[295]. Furthermore, in the R-parity-violating minimally supersymmetric SM (reviewed for example in ref. 296), the supersymmetric partners of quarks can have the properties of leptoquarks (examples of leptoquark interactions are shown in Fig. 1a,c,h).

Di-quarks

- Scalar bosons that are either triplets or sextets of $SU(3)_c$ and couple to a quark and an anti-quark. They are predicted by GUTs based on the E_6 symmetry group[297] and appear in the R-parity-violating minimally supersymmetric SM (example in Fig. 1g).

Z' bosons

- Neutral, heavy vector bosons. They can be singlets under $SU(2)_L$ but also the neutral component of an $SU(2)_L$ multiplet. These particles can be resonances of the SM Z, for example, Kaluza–Klein excitations of the SM W in composite[298] or extra-dimensional models[299], or originate from an abelian symmetry (such as $B-L$ (ref. 294)) or gauged flavour symmetries[300] (example in Fig. 1d).

W' bosons

- Electrically charged but quantum chromodynamics-neutral vector particles. They can have similar origins to Z' bosons but also come for a left-right symmetry[301].

Vector-like quarks

- For vector-like fermions in general, left-handed and right-handed fields have the same quantum numbers under the SM gauge group (unlike SM fermions) and can thus have masses independently of electroweak symmetry breaking, meaning that they can be arbitrarily heavy. They appear in GUTs[302], as resonances of SM fermions in composite or extra-dimensional models[303] and as the supersymmetric partners of SM vectors and scalars[304] (examples in Fig. 1b,e).

Vector-like leptons

- These particles can have similar origins to vector-like quarks. In addition, they are involved in the seesaw mechanisms (type I, refs. 305,306 and type III, ref. 307) used to give masses to the light active neutrinos, as required by neutrino oscillations.

New scalars

- Scalars could be supersymmetric partners of SM fermions[304], but scalar fields of different representations under the SM gauge group can also be added. The most common option here is a copy of the SM Higgs, an $SU(2)_L$ doublet with hypercharge 0, leading to a two-Higgs doublet model[308,309]. (Note that we do not include coloured scalars with the properties of di-quarks or leptoquarks here; example in Fig. 1f.)

Heavy gluons

- Heavy gluons, (G'), are similar to Z' bosons but charged under the strong interactions. They can arise from the breaking of a larger gauge group down to $SU(3)_c$ or be excitations of the SM gluons.

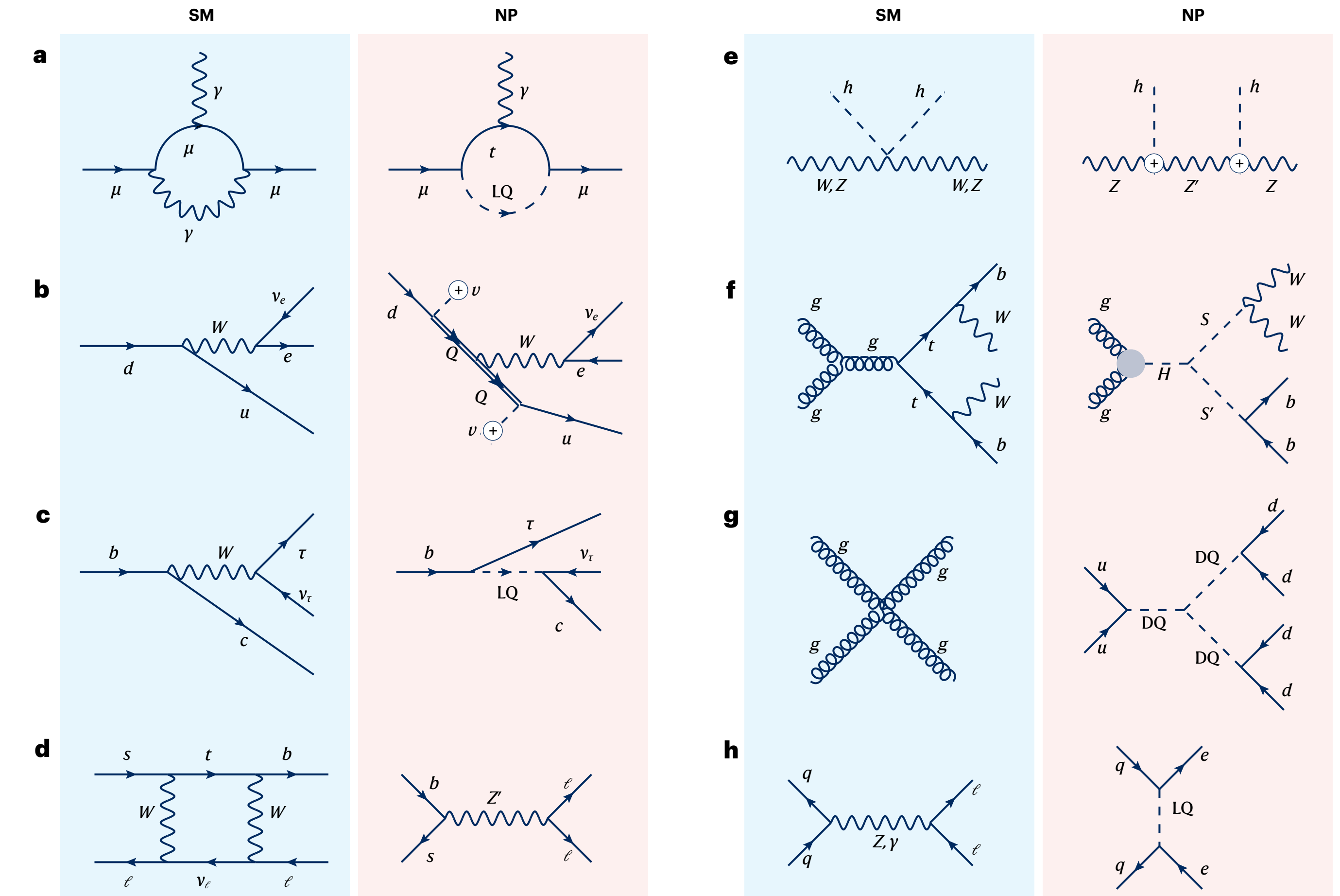

Fig. 1 | Feynman diagrams showing some of the processes in which anomalies are observed. In each panel, the left-hand diagram depicts the standard model (SM) process, and the right-hand diagram shows a possible new-physics (NP) explanation for the anomaly. **a**, Schwinger term contribution to a_μ and leptoquark (LQ) explanation. **b**, Leading β-decay contribution in the SM and modification via a vector-like quark (Q). **c**, W contribution to $R(D^{(*)})$ and leptoquark effect. **d**, W box contribution to $b \to s\ell^+\ell^-$ in the SM and Z' effect. **e**, $Z \to b\bar{b}$ and its modification via vector-like quarks. **f**, Top-pair production and decay in the SM and new Higgses that 'pollute' the measurement. **g**, Di-di-jet production in the SM and new-physics contribution via di-quarks (DQ). **h**, $pp \to e^+e^-$ in the SM and leptoquark contribution.

two vacuum expectation values of the two Higgs fields[27,28]. Other models with generic new scalars and fermions can also explain a_μ (refs. 29–32), as can an extended SM with two scalar leptoquarks, which address a_μ (Fig. 1a) via an m_t/m_μ enhancement[21,33,34] (in which m_t is the mass of the top quark and m_μ is the mass of the muon). This top mass enhancement also leads to interesting predictions for $h \to \mu^+\mu^-$ (ref. 35) and $Z \to \mu^+\mu^-$ (ref. 36) that can be measured at future colliders.

On the experimental side, the direct measurement of a_μ seems settled. But there will be updates of the SM predictions from $e^+e^- \to$ hadrons (for example, by Belle-II[37]), and the MUonE[38] experiment aims to independently determine the disputed SM contribution using a completely different method. Furthermore, lattice QCD simulations will deliver improved results within the next few years.

The anomalous magnetic moment of the tau is in principle very sensitive to new physics, but its measurement is very difficult. In fact, recent determinations are not even sensitive to the Schwinger term[39,40], and at present the only realistic option for reaching sufficient sensitivity to constrain new physics seems to be τ pair production at Belle-II using polarized beams[41].

The 17 MeV anomaly in excited nuclei decays

In an experiment on the proton capture process of lithium – ^{7}Li(p,e$^+$e$^-$)^{8}Be, conducted at the Atomki Laboratory, Hungary – measurements of the angle between the electron–positron pair emitted in the decay of the excited state to the ground state of beryllium showed an enhancement at an angle of 140° (ref. 42). Subsequently, similar enhancements were also seen in the decays of excited ^{4}He and ^{12}C nuclei[43,44]. The statistical significance exceeds 6σ in all cases. Although previous similar excesses[45] measured by the same collaboration at the Atomki Laboratory later disappeared[46], the current excess for lithium has been checked with different experimental setups, position-sensitive detectors and varying beam energies and appears at different angles with different target nuclei. The possibility of this being an SM effect is still not excluded[47] (a review of experimental and theoretical aspects of the anomaly can be found in ref. 48).

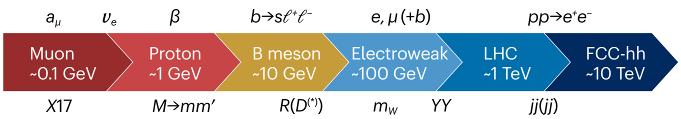

Fig. 2 | Compilation of various anomalies ordered according to the energy scale at which they appear. The existing Large Hadron Collider (LHC) reaches several teraelectronvolts; the Future Circular Collider using hadrons (FCC-hh) will, if built, push up the energy scale to several tens of teraelectronvolts.

However, if the explanation is new physics, then a particle with a mass of ~17 MeV is consistent with the angular measurements of both ^{8}Be and ^{4}He. From parity considerations (in the case that charge parity, *CP*, is conserved), only vector, axial-vector or pseudo-scalar states are possible. Interestingly, it is possible that this hypothetical '*X*17' boson could be related to $g-2$ of the muon[49] or to the neutron lifetime puzzle[50].

There is an effort to explore the *X*17 anomaly at various facilities. Resonant production of *X*17 through electron–positron annihilation in the Positron Annihilation into Dark Matter Experiment (PADME) at the Frascati National Laboratory, Italy, has been discussed[51]. A search for a new vector boson in the same mass range is planned at the Mu3e experiment[52], at the Paul Scherrer Institute (PSI), Switzerland. The New Judicious Experiments for Dark Sector Investigations (New JEDI) project has launched experiments at the ANDROMEDE facility at Orsay, France; the iThemba LABS accelerator and the half-AFRODITE detectors in Cape Town, South Africa, also plan *X*17 investigations[53]. Measurements are also possible at other facilities, such as CERN, Jefferson Lab in the USA, the Budker Institute in Novosibirsk, Russia and the MESA facility in Mainz, Germany[48].

Appearance and disappearance of electron neutrinos

All three generations of neutrino — electron neutrino, muon neutrino and tau neutrino — oscillate, changing their flavour from one type to another. Hence, in experiments, each type of neutrino can be seen to appear and disappear. Anomalies in neutrino appearance revolve around the excesses in quasi-elastic production of electrons from accelerator neutrinos reported by the LSND experiment[54] at Los Alamos National Laboratory, USA, and MiniBooNE[55] at Fermilab, USA. In particular, the MiniBooNE experiment (a Cherenkov detector) observed an excess in the neutrino energy range $200 < E_\nu < 1{,}250$ MeV with a significance of 4.8σ[56]. However, a reanalysis of the theoretical uncertainties led to a smaller tension with the SM prediction[57]. The MicroBooNE experiment (a liquid-argon time projection chamber, also at Fermilab) began operating in 2015 (ref. 58) and its results indicate that the MiniBooNE excess cannot be explained entirely by electron neutrino appearance[59].

A first combined analysis of the MiniBooNE and MicroBooNE data has been completed, in the context of the SM extended by the addition of a single 'sterile' neutrino (a neutrino that, in the absence of mixing, does not interact with SM gauge bosons): for MiniBooNE alone, there is a preference for this extended model over the SM of 4.6σ; the addition of the MicroBooNE exclusive electron-neutrino data reduces the significance to 4.3σ, and to 3.4σ for the inclusive data[60]. Once constraints are included from the MINOS experiment of Fermilab[61] and the IceCube Neutrino Observatory[62] in Antarctica, the preference for active–sterile neutrino mixing is further diminished[63]. Therefore, more exotic options for new physics, such as energy-dependent mixing parameters, have been considered[64] (reviewed elsewhere[65]).

Anomalies suggesting the disappearance of electron neutrinos and anti-neutrinos are observed in reactor neutrino experiments[66–68] and in the gallium radioactive-source experiments GALLEX[69,70] and SAGE[71]. The latter experiments use intense ^{51}Cr and ^{37}Ar radioactive sources and search for the inverse β reaction $\nu_e + {}^{71}\mathrm{Ga} \to {}^{71}\mathrm{Ge} + e^-$. The results indicate fewer ^{71}Ge occurrences than expected. The significance of the deficit is about 5σ and is referred to as the gallium anomaly[72,73]. Reference[74] critically evaluated the assumptions underlying the gallium anomaly and found several possible caveats (such as the gallium lifetime or neutrino flux) that could account for the excess without invoking new physics. A straightforward explanation in terms of active–sterile neutrino oscillations is excluded by solar and reactor neutrino experiments[75,76]. Therefore, one again has to resort to more exotic options, such as a parametric resonance[77] (reviewed elsewhere[74]).

The proposed explanations of the gallium anomalies can be tested through measurements that use a different neutrino source, such as ^{65}Zn at the BEST experiment[78] (Baksan Neutrino Observatory, Russia), and/or other detection materials (for example, ^{37}Cl). DUNE[79] and the Short Baseline Neutrino programme at Fermilab[80] will further scrutinize our understanding of neutrino oscillations.

β-Decay anomalies

The Cabibbo–Kobayashi–Maskawa (CKM) matrix, *V*, is a 3 × 3 matrix whose elements reflect the mixing between the generations of quark:

$$V = \begin{pmatrix} V_{ud} & V_{us} & V_{ub} \\ V_{cd} & V_{cs} & V_{cb} \\ V_{td} & V_{ts} & V_{tb} \end{pmatrix}. \tag{1}$$

The CKM matrix is by construction unitary[81], and therefore, as required, it conserves probability. It is known from experiments that it has a hierarchical structure; although the size of the diagonal elements is close to unity, the off-diagonal elements are small. The SM prediction that $\sum_j V_{ij} V^*_{jk} = \delta_{ik}$ can be tested experimentally. In this context, the Cabibbo angle[82], which parametrizes the mixing between the first two quark generations, is particularly interesting as it dominates the first and second row and column relations. In fact, there is a deficit in first-row and first-column CKM unitarity, which can be traced back to the fact that V_{ud} extracted from β-decays[83,84] (Fig. 1b) does not agree with V_{us} determined from kaon (*K*) and tau decays or V_{cd} from *D* meson decays. There is also a disagreement between the determinations of V_{us} from $K \to \mu\nu$ decays[85] and $K \to \pi\ell\nu$ decays[86]. The significance of these deviations crucially depends on the radiative (quantum) corrections to β-decays[84,87,88] and on the treatment of the tensions between kaon[89–91] and tau decays[92]. In summary, both tensions are slightly below the 3σ level.

A sub-per-mille effect suffices to explain these tensions. The disagreement between the two determinations of V_{us} can only be explained via a right-handed quark current, which points to vector-like quarks as the extension of the SM (Fig. 1b). The deficit in first-row and first-column CKM unitarity can be explained via left-handed (that is, SM-like) new physics in β-decays. An effect both in β-decays or in the Fermi constant G_F (determined from muon decay, $\mu \to e\nu\nu$, and which is needed to extract V_{ud}), is possible. There are four options[93]: first, a direct (tree-level) modification of β-decays; second, a direct (tree-level) modification of muon decay; third, a modified *W*-*μ*-*ν* coupling entering muon decay; and fourth, a modified *W*-*u*-*d* coupling entering β-decays (the effect of a modified *W*-*w*-*ν* drop out). The first option could in principle be realized by a *W*′ boson[94] or a leptoquark[95], although, in the case of the leptoquark, stringent bounds arise from other flavour observables. The second possibility can be achieved by adding a singly charged $SU(2)_L$ singlet scalar[96], a W' boson[94] or Z' boson with flavour violating couplings[97]. The last two options can be achieved by vector-like leptons[98,99] and vector-like quarks[100–103], respectively. However, without a compensating effect[104], explaining the Cabibbo angle anomaly via a modification of G_F increases the tension in the W mass.

There is also a significant tension (~4σ) between the neutron lifetime (and thus V_{ud}) determined from beam and bottle experiments — experiments that detect the β-decay products in a neutron beam or that count how many neutrons survive a certain time of confinement in a 'bottle'. The average of the beam values is $\tau_n = 888.2 \pm 2.0$ s (refs. 105,106), whereas the best determination from bottle experiments is $\tau_n = 877.75 \pm 0.28_{\rm stat} + 0.22/{-0.16}_{\rm syst}$ s (ref. 107). To understand the implications for new physics, it is important to remember that in bottle experiments the remaining neutrons are counted, but beam experiments count the protons from neutron decay. Therefore, if the branching ratio of neutrons to final states with protons is not 100%, the lifetime measured in beam experiments would be larger than the real neutron lifetime. The beam–bottle discrepancy cannot be explained within an EFT setup — that is, with heavy new physics — because this would lead to proton decay, which is very tightly constrained. However, neutron decay to light dark-matter particles could result in a stable proton for very fine-tuned mass configurations[108]. Alternatively, neutron oscillations into mirror neutrons have been proposed as an explanation[109].

Improved measurements and theory calculations of β-decays will be available in the coming years[110]. The NA62 experiment of CERN could measure the ratio $(K \to \mu\nu)/(K \to \pi\mu\nu)$ to assess the possibility of right-handed currents[91] and the PIONEER experiment of PSI will measure pion β-decay[111] to determine V_{us}, for which the theoretical prediction is accurate. The neutron–anti-neutron oscillation explanation of the lifetime puzzle can be tested at the PSI ultracold neutron source[112].

Hadronic meson decays

Several anomalies have been observed in the decay of mesons into two lighter mesons — including CP violation in $b \to s$ transitions and D meson decays, which is known to be suppressed in the SM, and total branching ratios for charged current B meson decays (CP is the combined application of charge conjugation C and parity transformation P (mirroring)). In the SM, CP is conserved by all interactions except transitions involving the single complex phase of the CKM matrix. CP violation is only induced via the W boson and is thus very small within the SM.

The improved SM predictions for the total branching ratios $\bar{B} \to D^{(*)}K$ and $\bar{B}_s \to D_s^{(*)}\pi$ (ref. 113), based on QCD factorization[114], deviate from the corresponding experimental measurements[6] with a combined significance of 5.6σ. However, because the anomaly is observed in total branching rates, there is no cancellation or suppression of QCD uncertainties, and the accuracy of the predicted SM values has been challenged[115]. These are charged current processes, mediated at the tree level in the SM, and it is particularly challenging to find a new-physics explanation for the anomaly, given that an $O(50\%)$ effect is needed. In fact, both W' models[116] and di-quark explanations are stringently constrained by LHC searches[117] because they can be produced resonantly at the LHC.

The first evidence for CP violation in D decays was observed in 2011 in the LHCb experiment[118] at CERN; the discovery level was reached in 2019, with the difference in CP asymmetries between $D \to KK$ and $D \to \pi^+\pi^-$ given by $\Delta A_{CP}^{\rm LHCb} = (-15.4 \pm 2.9) \times 10^{-4}$ (ref. 119). This has to be compared with the SM prediction, which is notoriously difficult to estimate for charm-quark physics, of $|\Delta A_{CP}^{\rm LHCb}| < 3.6 \times 10^{-4}$ (ref. 120). The CP asymmetry in $D \to K^+K^-$ has been determined directly[121], which enables a test of U-spin symmetry in the SM and shows indications that it is violated[122]. (Isospin symmetry uses the fact that for strong interactions, up and down quarks are, to a good approximation, indistinguishable as they are very light: U-spin symmetry extends this concept to include strange quarks. However, as the strange quark is much more massive than first-generation quarks, the symmetry is more strongly broken and the resulting predictions are less reliable.) An overview of new-physics explanations for CP asymmetries in D decays is given in ref. 123, including the possibilities of Z' bosons and di-quarks — although note that limits on these have since got much more stringent.

There are also hints of BSM CP violation in hadronic B meson decays with $b \to s$ transitions, including the long-standing $B \to K\pi$ puzzle[124], which was confirmed by LHCb[125]. Here, the theory predictions within the SM seem to be more reliable as they use isospin relations[126]; the significance is around 3σ but it is supported by $B_s \to KK$ measurements[127]. Finally, although not CP-violating, there are indications of U-spin violation in polarization observables[128]. To explain these hints of BSM CP violation, smaller new-physics effects are required than for the total branching ratios or the polarization observables, making an explanation based on Z' bosons or heavy gluons more favourable but still not straightforward[129]; constraints on di-quark models are expected to be less stringent.

Progress on the SM side does not seem easy. However, a lot of data is expected from LHCb and Belle-II at KEK, Japan. Furthermore, the hints of CP violation in B and D decays could be related to direct CP

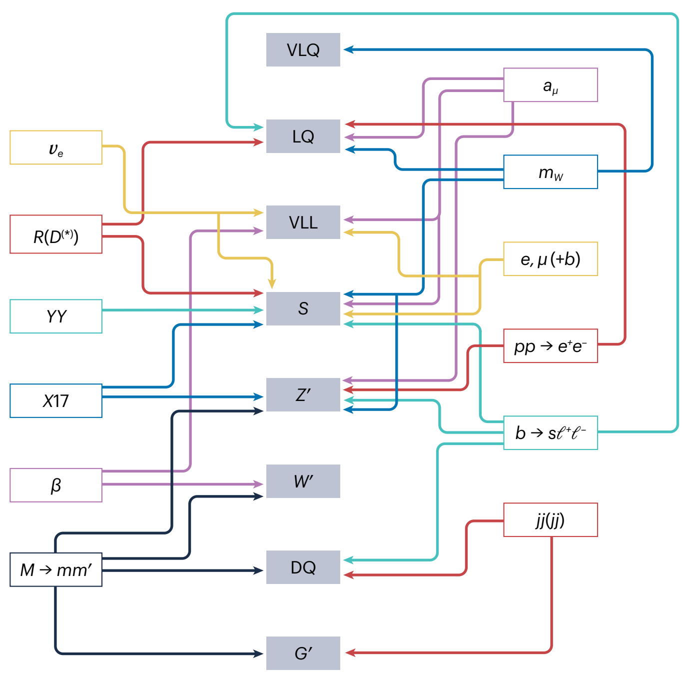

Fig. 3 | Implications of anomalies for extending the standard model with new particles. For each of the anomalies discussed in this Review, arrows indicate which extension of the standard model could be the explanation: vector-like quarks (VLQ), leptoquarks (LQ), vector-like leptons (VLL), electrically neutral scalars (S), neural gauge bosons (Z'), charged gauge bosons (W'), di-quarks (DQ) and heavy gluons (G').

Table 1 | Summary of final states seen in multilepton anomalies at the Large Hadron Collider

Final state	Characteristics	SM backgrounds	Significance
$\ell^+\ell^-$+(b-jets)[225,228,229]	$m_{\ell\ell}$<100 GeV	$t\bar{t}$, Wt	>5σ
$\ell^+\ell^-$+(no jet)[224,286]	$m_{\ell\ell}$<100 GeV	W^+W^-	≈3σ
$\ell^\pm\ell^\pm$, 3ℓ + (b-jets)[227,287,288]	Moderate Higgs transverse mass	$t\bar{t}W^\pm$, $t\bar{t}t\bar{t}$	≈3σ
$\ell^\pm\ell^\pm$, 3ℓ, (no b-jet)[226,289,290]	In association with h	$W^\pm h(125)$, WWW	≳4σ
$Z(\to\ell\ell)\ell$, (no b-jet)[225,291]	p_T^Z < 100 GeV	$ZW^\pm$	>3σ

violation in the kaon system $(\varepsilon'/\varepsilon)$[130] (see ref. 131 for an overview of ε'/ε) and U-spin violation[132].

Charged-current tauonic *B* decays

These charged-current transitions — mediated at the tree level by a W boson in the SM (Fig. 1c) — have significant branching ratios, up to $O(10^{-2})$. With light leptons, they are used to extract the CKM element V_{cb} and the result is consistent with the global CKM fit[133,134]. (Note that there is also a long-lasting tension in the inclusive versus exclusive determination of V_{cb}[135] (and V_{ub}) in which $B\to D^{(*)}\ell\nu$ is involved. However, it has been shown that this anomaly cannot be explained by new physics[136].) The ratios (of branching) $R(D^{(*)}) = \mathrm{Br}(B\to D^{(*)}\tau\nu)/\mathrm{Br}(B\to D^{(*)}\ell\nu)$ are measured to be approximately 20% bigger than the SM predictions, resulting in a ≳3σ significance[92] for new physics related to tau leptons. Analyses from BaBar[137,138], Belle[139–143] and LHCb[144–146] used different tag and tau reconstruction methods — the online update of ref. 92 provides an overview.

This transition occurs at the tree level in the SM. Therefore, also a tree-level new-physics effect is necessary to obtain the needed effect of $O(10)$% with respect to the SM (assuming heavy new physics with perturbative couplings). Therefore, charged Higgses[147–149], W' bosons[150] (with or without right-handed neutrinos) or leptoquarks[34,151–153] are candidates. Although there is a small region in parameter space left that can account for $R(D^{(*)})$ with charged Higgses[154,155], LHC searches constrain W' solutions[150,156], leaving leptoquarks as the probably best solutions (Fig. 1c). However, leptoquark constraints from $B_s-\bar{B}_s$ mixing, $B\to K^{(*)}\nu\nu$ and LHC searches must also be respected, with the result that the $SU(2)_L$ singlet vector leptoquark[157–163] or the singlet–triplet model[164–166] is particularly interesting.

Concerning future prospects, $R(D^{(*)})$ and related ratios can be measured at Belle-II[37], by LHCb using Run 3 data and using the parked B data from CMS[167]. Polarization observables will be measured so precisely that they will distinguish between different models for new physics, and an improvement in the form factors from lattice QCD is expected.

Flavour-changing neutral-current semi-leptonic *B* decays

Similar to all flavour-changing neutral-current processes, $b\to s\ell^+\ell^-$ transitions are 'loop suppressed' within the SM (by the small probability that two particles are produced via quantum fluctuations and annihilate again), because only the couplings of the charged W can violate quark flavour (Fig. 1d). This results in small branching ratios, up to a few times 10^{-6}. Although previous hints[168] for lepton flavour universality violation in the ratios $R(K^{(*)}) = \mathrm{Br}(B\to K^{(*)}\mu^+\mu^-)/\mathrm{Br}(B\to K^{(*)}e^+e^-)$ were not confirmed[169] and $B_s\to\mu^+\mu^-$ (refs. 170,171) now agrees quite well with the SM prediction[172,173], there are several $b\to s\mu^+\mu^-$ observables that deviate significantly from the SM predictions. These include the angular observable P_5' (refs. 174,175), the total branching ratio $\mathrm{Br}(B\to K\mu^+\mu^-)$[176,177], $\mathrm{Br}(B_s\to\phi\mu^+\mu^-)$[178,179] and also semi-inclusive observables[180]. As a result, global fits find a preference for new physics at the 5σ level[181–183]. Recently, the Belle-II collaboration reported an 2.8σ excess over the SM hypothesis in the closely related $B\to K^*\nu\bar{\nu}$ decay[184].

The new measurements of $R(K^{(*)})$ require new physics with lepton flavour universality, and $B_s\to\mu\mu$ constrains axial couplings to leptons. Such a new-physics effect at the required level of $O(20\%)$ (with respect to the SM) can be most naturally obtained in the following ways[185]. The first possibility is a Z' boson with lepton-flavour-universal couplings but flavour-violating couplings to bottom and strange quarks[186,187] (Fig. 1d). However, owing to the bounds from $B_s-\bar{B}_s$ mixing[188], from the LHC (see, for example, ref. 189) and from LEP[190], a full explanation requires some tuning in $B_s-\bar{B}_s$ mixing by a right-handed sb coupling[191] or a cancellation with Higgs contributions[192]. Furthermore, $K^0-\bar{K}^0$ and $D^0-\bar{D}^0$ mixing requires an approximate global $U(2)$ flavour symmetry[129]. The second possibility is a τ or charm loop effect, via an off-shell photon penguin[193]. The leptoquark representations which can give rise to such a tau loop are the S_2 leptoquark[194], the U_1 leptoquark[195] or the combination of leptoquarks S_1+S_3 (ref. 165). The two-Higgs-doublet model with generic flavour structure[196] can generate the desired effect via a charm loop C_9^U (refs. 197,198). Alternatively, a di-quark solution is possible[199].

The best hope to solve the bottleneck for SM predictions is to improve lattice calculations over the full range of momentum transfer (q^2), as performed in ref. 177, and to combine them with other non-perturbative methods such as dispersion relations[200]. Or the experimental side, again Belle-II, LHCb and the parked B programme of CMS will help to resolve the situation.

Mass of the *W* boson

In general, three parameters are sufficient to parameterize completely (at the tree level) the electroweak sector of the SM. They are usually taken to be the Fermi constant G_F, the fine-structure constant α and the mass of the Z boson as these are measured most precisely. In this input scheme, the W mass is not a free parameter but can be calculated as a function of G_F, α and m_Z (and the Higgs and the top mass that enter at the loop level). The CDF II result[201] from Fermilab shows a very strong 7σ tension with the SM prediction. However, LHC[202–205] results and those from the predecessor of the LHC, the Large Electron–Positron collider (LEP)[206], are closer to the SM, only 1.8σ away, and are thus in tension with the CDF II value. Using a conservative error estimate, following the Particle Data Group recommendation[6], the combined result shows a tension of 3.7σ with the SM[207]. (This average does not include the latest ATLAS result[208], which supersedes ref. 202, however doing so has a small impact on the fit.) Within the electroweak fit, there are also tensions owing to the forward–backward asymmetry measurement in $Z\to b\bar{b}$ (ref. 209) (≈2σ) and in the lepton asymmetry parameter A_ℓ (ref. 207), mainly owing to the electron channel.

The tension in the W mass is most easily explained by a tree-level effect, for example, an $SU(2)_L$ scalar triplet that acquires a vacuum expectation value[210] or via $Z-Z'$ mixing (Fig. 1e) in the case that Z' is an $SU(2)_L$ singlet[211]. However, loop effects of new particles with masses below or at the teraelectronvolt scale — such as vector-like quarks[212] or leptoquarks[213] — are possible as well[214].

At a hadron collider, an increase in the instantaneous luminosity — as will happen with the upgraded high-luminosity LHC from 2029 — makes the measurement of the W mass more difficult (although LHCb should still be able to contribute because it is configured such that it does not use the full LHC instantaneous luminosity). Very precise results would, however, be possible from a future electron–positron collider (such as the International Linear Collider (ILC)[215], the Compact Linear Collider (CLIC)[216,217], the Future Circular Collider with electrons and protons (FCC-ee)[218,219] or the Circular Electron Positron Collider (CEPC)[220,221]), and these could also improve significantly on the precision of the input parameters for the electroweak fit.

Multilepton anomalies at the LHC

The so-called multilepton anomalies are LHC processes that have two or more leptons in the final state (reviewed elsewhere[222]), and for which statistically significant disagreements with the SM predictions have been observed[223–228]. The final states might contain b-jets (because quarks and gluons are confined at low energies, they do not appear as free particles in a detector but rather hadronize and leave signatures called jets; a b-jet is a jet that contains a bottom quark). Some of the excesses already emerged in the Run-1 data (2010–2013) of ATLAS and CMS[223,224]. They were confirmed[225,226,229] using the independent and larger data sets of Run 2 (refs. 225,226,229), leading to disagreements with the SM that exceed the 5σ threshold (Table 1). The fact that the leptons in these channels are non-resonant (that is, there is no peak in the invariant mass spectrum) shows that, at least within the SM, they are related to leptonic W decays.

These excesses correspond to Higgs-like signatures ($h \to WW$), which are experimentally robust. On the theoretical side, higher-order QCD and electroweak corrections have been calculated for the main SM backgrounds. Most prominently, next-to-next-to-leading-order QCD corrections are available for leptonic observables in $t\bar{t}$ distributions[230], non-resonant W^+W^- (refs. 231–235), $ZW^\pm$ (ref. 236), Wh (refs. 237–239) and $t\bar{t}W^\pm$ (ref. 240) production. Electroweak corrections are also available at next-to-leading order and are small for Higgs-like signals[241–245]. The description of the data by the SM outside these Higgs-like regions is within the residual errors.

A particularly significant disagreement is observed in differential lepton distributions in $t\bar{t}$ measurements[225,228] (Fig. 1f). For all SM simulations used, ATLAS finds such a high χ^2 value that they conclude[229]: "No model (SM simulation) can describe all measured distributions within their uncertainties." Although this effect warrants further investigation of the SM predictions, it is important to note that excesses also appear in WW signatures without jets (in which SM $t\bar{t}$ production is strongly suppressed) and in $Wh/3W$, $t\bar{t}W$, $t\bar{t}t\bar{t}$ and ZW production with low Z boson transverse momentum (p_T^Z), which indicates that the excess is probably not due to a mismodelling of the SM $t\bar{t}$ production and decay. (In addition, there is a hint for a resonant $t\bar{t}$ excess at around 400 GeV (ref. 246), with a local significance of 3.5σ and a global significance of 1.9σ.)

Table 2 | Experimental and theoretical features of anomalies, indicating which are favourable and unfavourable for further investigation

Anomaly	Favourable	Unfavourable
Anomalous magnetic moment of the muon, a_μ	Precise and confirmed direct measurements	Standard model (SM) prediction plagued by hadronic uncertainties; tensions within $e^+e^- \to$ hadrons measurements and with lattice quantum chromodynamics; quite large new-physics effect needed, model building is challenging
The 17 MeV anomaly in excited nuclei decays, X17	High statistical significance	Only observed by a single experiment (despite different settings); possibility of not-understood nuclear effects
Appearance and disappearance of electron neutrinos, ν_e	High statistical significance; observed by different experiments	Theory errors might be underestimated; explanation by sterile-neutrino mixing excluded by other experiments
β-Decay anomalies, β	Natural place to search for new physics as only a sub-per-mille effect with respect to the SM is needed	Only one (competitive) measurement of $K \to \mu\nu$ available; β-decays need hadronic theory input to extract V_{ud}; lifetime difference can only be explained by exotic new physics
Hadronic meson decays, $M \to mm'$	Many different channels	SM plagued by hadronic effects; new-physics explanations challenged by searches at the Large Hadron Collider (LHC)
Charged-current tauonic B decays, $R(D^{(*)})$	Measurements from different collaborations; small theory uncertainty; possible connection to $b \to s\ell^+\ell^-$	Difficult measurement; limited significance; large effect needed, model building is challenging
Flavour-changing neutral-current semi-leptonic B decays ($b \to s\ell^+\ell^-$)	Many different observables measured; consistent picture; large significance; possible connection to $b \to c\tau\nu$	Sensitive to form factors and other hadronic inputs
W mass, m_W	Theoretically clean; statistically significant; very sensitive to new physics, many natural new-physics explanations	Tensions among the measurements
LHC multilepton anomalies, $e\mu(+b)$	Statistically very significant; large multiplicity of signatures; coherent picture; consistent with the Higgs-like signals	Some of the SM predictions can be difficult; complex SM extension needed
Higgs-like signal, YY	Statistically significant; many different channels; motivated by the multilepton anomalies	Possible look-elsewhere effect
Di-jet and di-di-jet resonances, $jj(jj)$	Agreement between different measurements	Poor mass resolution; challenging theory explanation
Non-resonant di-electrons, $q\bar{q} \to e^+e^-$	Agreement between ATLAS and CMS; ratio theoretically clean	Limited statistics; electrons are difficult LHC signatures

Table 3 | Anomalies assessed (positively, negatively or neutrally) against various criteria

Anomaly	Experimental signature	Experimental consistency	SM prediction	Statistical significance	New-physics explanation	Consistent connection
a_μ	+	0*	–	+	0	–
$X17$	+	0	–	+	0	0
ν_e	–	0	–	+	–	–
β	+	0	0	–	+ (–)**	+
$M\to mm'$	0	+	–	0	–	0
$b\to s\ell^+\ell^-$	+	+	0	+	0	+
$R(D^{(*)})$	–	+	+	–	–	+
m_W	0	–	+	+	+	+
$e\mu\,(+b)$	0	+	0	+	0	+
$\gamma\gamma$	+	+	+	0	+	+
$jj(jj)$	0	+	+	0	0	–
$pp\to e^+e^-$	0	+	+	–	0	–

*Note that although the results of the Brookhaven and Fermilab experiments for a_μ agree very well, the neutral rating is due to the inconsistencies between the experiments measuring $e^+e^-\to$hadrons, which are used for calculating the SM prediction via dispersion relations. **The first assessment refers to the deficit in Cabibbo–Kobayashi–Maskawa unitarity and the V_{us} disagreement and the second one in brackets refers to the lifetime difference.

The multilepton anomalies can be explained by the associated production of new scalars – that is, via the decay of a heavier scalar into two lighter ones. In particular, the deviations from the SM predictions in the differential distributions of leptons from $t\bar{t}$ decays can be resolved by the production of a new neutral Higgs, H, that decays into two lighter ones S and S', which subsequently decay to W bosons and b quarks, respectively[228] (Fig. 1f). This setup is preferred over the SM hypothesis by more than 5σ and points towards $m_S \approx 150$ GeV. Similarly, the excess in $h\to WW$ can be described by a new Higgs boson decaying to WW (refs. 224,247), and the same-sign lepton signals with b jets by the associated production of H with top quarks, where again $H\to SS'\to WWbb$ (ref. 225).

Given the very large statistical significance of many channels in the multilepton anomalies (more than 8σ for the simplified model of ref. 225), the focus for the Run-3 data (2022–2025) will shift to those signatures that are currently statistically limited. For instance, the study of the differential $\ell^+\ell^-$ distributions with a full jet veto, or $\ell^\pm\ell^\pm$ with and without a b-jet, would profit from more data. On the theory side, merging full next-to-next-to-leading-order calculations[230] and including off-shell effects[248] with parton showers at the same accuracy would significantly improve the SM simulations.

Higgs-like resonant signals

New particles that are directly produced at colliders show up as bumps in the otherwise continuous invariant mass spectrum of the corresponding decay products. For finding new scalar bosons, di-photon ($\gamma\gamma$) distributions are very sensitive: although they have, in general, small rates because they are loop-suppressed, the experimental signature is very clear. In fact, there are several hints for di-photon resonances at 95 GeV (refs. 249,250), at ~152 GeV (ref. 251; the mass of this excess is consistent with the invariant mass of di-leptons in the multilepton anomalies) and also at ~680 GeV (refs. 252,253). The hint at 95 GeV is supported by a di-tau excess reported by CMS[254] (although it is not confirmed by ATLAS[255]), and a ZH signal (with $H\to b\bar{b}$) by LEP[256], as well as the WW channel[224,247]. The $\gamma\gamma$ (plus missing energy) hint at 152 GeV is supported by several signals in associated production[251,257], including WW plus missing energy[247]. Combining all channels, global significances of 3.8σ and 3.9σ are found for 95 GeV (ref. 258) and 152 GeV (ref. 259), respectively – if, for the latter, a simplified model with $pp\to H\to SS^*$ is assumed. (Note that ref. 258 updated the results of ref. 259 by including additional new excesses, further increasing the significance of the narrow excess at around 152 GeV.)

There are also hints, around 3σ each[260], of a new scalar in di-photon and di-Z searches with a mass around 680 GeV (refs. 253,261). Taking into account the resolution of these measurements, these signals are compatible with the 3.8σ local and 2.8σ global excess in $bb\gamma\gamma$ at around 650 GeV (ref. 262; in which the $b\bar{b}$ invariant mass is compatible with 95 GeV) and the WW excess[263] in vector–boson fusion. (Vector–boson fusion means that the new scalar is radiated from a Z or W pair. At the LHC, this leads to the formation of two forward jets, close to the beamline.) ATLAS sees an excess in $A\to H+Z$ (with $H\to b\bar{b}, t\bar{t}$) for masses $m_A \approx 650$ GeV and $m_H \approx 450$ GeV; the local significance is 2.85σ, globally 2.35σ. However, the interest in $bb\gamma\gamma$ is diminished by the non-observation[264] of an excess in $\tau\tau\gamma\gamma$, and the WW excess cannot be fully explained within a model[265].

These hints for resonances point towards the extension of the Higgs sector of the SM, because only scalars can decay to photons. For the 95 GeV excess, at least an $SU(2)_L$ doublet[266], triplet[267] or even a more complex scalar sector is needed[268]. To also address the di-Higgs excess, 650 GeV $\to b\bar{b}$(90 GeV) + $\gamma\gamma$(125 GeV), resonant pair production of the SM Higgs and a new scalar are required[269]. For the 152 GeV excess, an even larger scalar sector is necessary because the bulk of the signal is in associated production. In fact, not only are the most significant excesses related to missing energy, the WW signal can also be explained for $m_S \approx 150$ GeV – the decay chain $pp\to H\to(S\to\gamma\gamma, WW)+(S'\to\text{invisible})$ describes data well. In general, a quite complicated scalar sector is suggested, such as an extended Georgi–Machacek model[270,271] or excitations of the SM Higgs[272].

Given the current strength of the excesses, Run 3 of the LHC (and definitely the high-luminosity LHC[273]) should suffice to verify or falsify the existence of these particles. To fully explore their properties, however, an e^+e^- accelerator could be required.

Di-jet and di-di-jet resonances

A particle decaying into two quarks (or two gluons) results in a di-jet (jj) signature in LHC detectors. ATLAS[274] has observed a weaker limit than expected if there were no new physics in resonant di-jet searches slightly below 1 TeV. CMS[275] has found hints for (non-resonant) pair production of di-jet resonances at a mass of ~950 GeV with a local significance of 3.6σ (2.5σ globally). This compatibility suggests that both excesses might be due to the same new particle, X, either produced directly (resonantly) in proton–proton collisions ($pp \to X \to jj$), or pair-produced via a new state Y in the process $pp \to Y^{(*)} \to XX \to (jj)(jj)$. In fact, ref. 276 finds a global 3.2σ significance at $m_Y \approx 3.6$ TeV. In the latest analysis, ATLAS finds a di-(di-jet) excess[277] at ~3.3 TeV with a di-jet mass of 850 GeV, which could be compatible with a similar excess from CMS (once the poorer jet-energy resolution is taken into account). Furthermore, there is a slight excess in tb searches at ~3.5 TeV (ref. 278).

For explanations, two options come to mind[276]: two scalar di-quarks (Fig. 1g) or new massive gluons seem to be the most plausible candidates. The first could explain the tb excess; a specific realization of the second is based on an $SU(3)_1 \times SU(3)_2 \times SU(3)_3$ gauge group, broken down to $SU(3)$ colour via two bi-triplets.

Non-resonant di-electrons

If the mass of a particle is higher than the energy reach of a collider, its impact can still be seen by looking at the high-energetic end of the spectrum of a distribution. There, the effects of virtual particles are most relevant because they possess a relative enhancement with respect to the SM. In such a non-resonant search for highly energetic, oppositely charged leptons (Fig. 1h), CMS and ATLAS observe more electrons than expected according to the SM (refs. 279,280). Because the number of observed muons is compatible with the SM prediction, this is a sign of a violation of lepton flavour universality, and the ratio of muons to electrons provided by CMS has the advantage of reduced theoretical uncertainties[281]. Performing a model-independent fit, it is seen that new physics at a scale of 10 TeV with order-one couplings can improve over the SM hypothesis by ~3σ (ref. 282).

As this analysis involves non-resonant electrons that do not originate from the on-shell production of a new particle, the scale of the new physics must be higher than the energy scale of the LHC (or be produced non-resonantly like leptoquarks). This can be achieved with new physics at the 10 TeV scale with order-one coupling to first-generation quarks and electrons[103]. Therefore, Z' bosons[283] or leptoquarks[95] (Fig. 1h) have the potential to explain the CMS measurement. Data from LHC Run 3 should suffice to determine the validity of these excesses.

Comparisons and outlook

It cannot be expected that all anomalies will be confirmed, but it is also statistically unlikely that all will disappear. It is thus important to investigate the implications of these anomalies for new physics, to assess possible correlations among them and identify experimental signatures that should be sought for future verification (or falsification).

Experimental and theoretical features of each anomaly that we have discussed above are given in Table 2, in terms of which are favourable or unfavourable to further examination. (Note that, although we have tried to be objective here, the impact of personal opinion is unavoidable.)

The anomalies are also compared in Table 3, according to the several criteria defined by the following questions:

- Experimental signature: is the experimental environment clean? Is the signal well separated from the background?
- Experimental consistency: do multiple independent measurements exist? Are they in agreement with each other?
- SM prediction: how accurate and reliable is the SM prediction? Are the results conflicting?
- Statistical significance: how sizable are the deviations from the SM predictions?
- New-physics explanation: are there models that can naturally account for the anomaly? Are they in conflict with other observables?
- Consistent connection: are there connections to other anomalies via the same new particle or model? How direct is this connection?

Symbols in Table 3 represent an assessment of these criteria that is positive (+), negative (−) or neutral (0) — meaning in this last case that positive and negative aspects compensate to a good approximation.

Figure 3 summarized which extensions of the SM are indicated by each of the anomalies we have discussed here. It is clear that many of the anomalies point towards new Higgs-like scalars. In particular, the agreement between the mass of the scalar suggested by the multilepton anomalies and the $\gamma\gamma$ excess around 152 GeV is striking. Leptoquarks are also interesting candidates and, in particular, enable a combined and correlated explanation of $b \to c\tau\nu$ and $b \to s\ell^+\ell^-$ via the tau loop[284,285]. Finally, $Z \to b\bar{b}$, m_W and the Cabibbo angle anomaly could be explained by vector-like quarks. Of course, many more possible connections exist, as seen in Fig. 3, suggesting that there are many interesting directions for future research.

Particle physics is a very exciting area. Although the SM has been consolidated over the past five decades, hints of new particles and new interactions are still emerging. These hints originate from different experiments and range over many orders of magnitude in energy, making it a challenging task to find combined explanations for the anomalies. Not all anomalies will be confirmed by ongoing and forthcoming experimental efforts, but establishing just one of these hints beyond reasonable doubt would lead particle physics into a new era, the age of BSM physics.

Published online: 19 March 2024

References

1. Higgs, P. W. Broken symmetries, massless particles and gauge fields. *Phys. Lett.* **12**, 132–133 (1964).
2. Englert, F. & Brout, R. Broken symmetry and the mass of gauge vector mesons. *Phys. Rev. Lett.* **13**, 321–323 (1964).
3. Aad, G. et al. Observation of a new particle in the search for the Standard Model Higgs boson with the ATLAS detector at the LHC. *Phys. Lett. B* **716**, 1–29 (2012).
4. Chatrchyan, S. et al. Observation of a new boson at a mass of 125 GeV with the CMS experiment at the LHC. *Phys. Lett. B* **716**, 30–61 (2012).
5. Aalbers, J. et al. First dark matter search results from the LUX-ZEPLIN (LZ) experiment. *Phys. Rev. Lett.* **131**, 041002 (2023).
6. Workman, R. L. et al. Review of particle physics. *PTEP* **2022**, 083C01 (2022).
7. Schwinger, J. S. On quantum electrodynamics and the magnetic moment of the electron. *Phys. Rev.* **73**, 416–417 (1948).
8. Bennett, G. W. et al. Final report of the muon E821 anomalous magnetic moment measurement at BNL. *Phys. Rev. D* **73**, 072003 (2006).
9. Abi, B. et al. Measurement of the positive muon anomalous magnetic moment to 0.46 ppm. *Phys. Rev. Lett.* **126**, 141801 (2021).
10. Aguillard, D. P. et al. Measurement of the positive muon anomalous magnetic moment to 0.20 ppm. *Phys. Rev. Lett.* **131**, 161802 (2023).
11. Aoyama, T., Kinoshita, T. & Nio, M. Theory of the anomalous magnetic moment of the electron. *Atoms* **7**, 28 (2019).
12. Colangelo, G., Hoferichter, M. & Stoffer, P. Two-pion contribution to hadronic vacuum polarization. *J. High Energy Phys.* **02**, 006 (2019).
13. Davier, M., Hoecker, A., Malaescu, B. & Zhang, Z. A new evaluation of the hadronic vacuum polarisation contributions to the muon anomalous magnetic moment and to $\alpha(m_Z^2)$. *Eur. Phys. J. C* **80**, 241 (2020) (Erratum: *Eur. Phys. J. C* **80**, 410 (2020)).

14. Keshavarzi, A., Nomura, D. & Teubner, T. $g-2$ of charged leptons, $\alpha(M_Z^2)$, and the hyperfine splitting of muonium. *Phys. Rev. D* **101**, 014029 (2020).
15. Borsanyi, S. et al. Leading hadronic contribution to the muon magnetic moment from lattice QCD. *Nature* **593**, 51–55 (2021).
16. Ignatov, F. V. et al. Measurement of the $e^+e^-\to\pi^+\pi^-$ cross-section from threshold to 1.2 GeV with the CMD-3 detector. Preprint at https://arxiv.org/abs/2302.08834 (2023).
17. Stoffer, P., Colangelo, G. & Hoferichter, M. Puzzles in the hadronic contributions to the muon anomalous magnetic moment. *J. Instrum.* **18**, C10021 (2023).
18. Hanneke, D., Fogwell, S. & Gabrielse, G. New measurement of the electron magnetic moment and the fine structure constant. *Phys. Rev. Lett.* **100**, 120801 (2008).
19. Aoyama, T., Kinoshita, T. & Nio, M. Revised and improved value of the QED tenth-order electron anomalous magnetic moment. *Phys. Rev. D* **97**, 036001 (2018).
20. Laporta, S. High-precision calculation of the 4-loop contribution to the electron $g-2$ in QED. *Phys. Lett. B* **772**, 232–238 (2017).
21. Crivellin, A., Hoferichter, M. & Schmidt-Wellenburg, P. Combined explanations of $(g-2)_{\mu,e}$ and implications for a large muon EDM. *Phys. Rev. D* **98**, 113002 (2018).
22. Athron, P. et al. New physics explanations of a_μ in light of the FNAL muon $g-2$ measurement. *J. High Energy Phys.* **09**, 080 (2021).
23. Ma, E., Roy, D. P. & Roy, S. Gauged $L_\mu-L_\tau$ with large muon anomalous magnetic moment and the bimaximal mixing of neutrinos. *Phys. Lett. B* **525**, 101–106 (2002).
24. Baek, S., Deshpande, N. G., He, X. G. & Ko, P. Muon anomalous $g-2$ and gauged $L_\mu-L_\tau$ models. *Phys. Rev. D* **64**, 055006 (2001).
25. Lees, J. P. et al. Search for a muonic dark force at BABAR. *Phys. Rev. D* **94**, 011102 (2016).
26. Czank, T. et al. Search for $Z'\to\mu^+\mu^-$ in the $L_\mu-L_\tau$ gauge-symmetric model at Belle. *Phys. Rev. D* **106**, 012003 (2022).
27. Everett, L. L., Kane, G. L., Rigolin, S. & Wang, L.-T. Implications of muon $g-2$ for supersymmetry and for discovering superpartners directly. *Phys. Rev. Lett.* **86**, 3484–3487 (2001).
28. Feng, J. L. & Matchev, K. T. Supersymmetry and the anomalous magnetic moment of the muon. *Phys. Rev. Lett.* **86**, 3480–3483 (2001).
29. Czarnecki, A. & Marciano, W. J. The muon anomalous magnetic moment: a Harbinger for 'new physics'. *Phys. Rev. D* **64**, 013014 (2001).
30. Kannike, K., Raidal, M., Straub, D. M. & Strumia, A. Anthropic solution to the magnetic muon anomaly: the charged see-saw. *J. High Energy Phys.* **02**, 106 (2012) (Erratum: *J. High Energy Phys.* **10**, 136 (2012)).
31. Kowalska, K. & Sessolo, E. M. Expectations for the muon $g-2$ in simplified models with dark matter. *J. High Energy Phys.* **09**, 112 (2017).
32. Crivellin, A. & Hoferichter, M. Consequences of chirally enhanced explanations of $(g-2)_\mu$ for $h\to\mu\mu$ and $Z\to\mu\mu$. *J. High Energy Phys.* **07**, 135 (2021) (Erratum: *J. High Energy Phys.* **10**, 030 (2022)).
33. Djouadi, A., Kohler, T., Spira, M. & Tutas, J. (e b), (e t) type leptoquarks at e p colliders. *Z. Phys. C* **46**, 679–686 (1990).
34. Bauer, M. & Neubert, M. Minimal leptoquark explanation for the $R_{D^{(*)}}$, R_K, and $(g-2)_\mu$ anomalies. *Phys. Rev. Lett.* **116**, 141802 (2016).
35. Crivellin, A., Mueller, D. & Saturnino, F. Correlating $h\to\mu\mu$ to the anomalous magnetic moment of the muon via leptoquarks. *Phys. Rev. Lett.* **127**, 021801 (2021).
36. Coluccio Leskow, E., D'Ambrosio, G., Crivellin, A. & Müller, D. $(g-2)\mu$, lepton flavor violation, and Z decays with leptoquarks: correlations and future prospects. *Phys. Rev. D* **95**, 055018 (2017).
37. Altmannshofer, W. et al. The Belle II physics book. *PTEP* **2019**, 123C01 (2019). (Erratum: *PTEP* **2020**, 029201 (2020)).
38. Abbiendi, G. et al. Measuring the leading hadronic contribution to the muon $g-2$ via μe scattering. *Eur. Phys. J. C* **77**, 139 (2017).
39. Aad, G. et al. Observation of the $\gamma\gamma\to\tau\tau$ process in Pb+Pb collisions and constraints on the τ-lepton anomalous magnetic moment with the ATLAS detector. *Phys. Rev. Lett.* **131**, 151802 (2023).
40. Haisch, U., Schnell, L. & Weiss, J. LHC tau-pair production constraints on a_τ and d_τ. *SciPost Phys.* **16**, 048 (2024).
41. Crivellin, A., Hoferichter, M. & Roney, J. M. Toward testing the magnetic moment of the tau at one part per million. *Phys. Rev. D* **106**, 093007 (2022).
42. Krasznahorkay, A. J. et al. Observation of anomalous internal pair creation in Be8 : a possible indication of a light, neutral boson. *Phys. Rev. Lett.* **116**, 042501 (2016).
43. Krasznahorkay, A. J. et al. New anomaly observed in He4 supports the existence of the hypothetical X17 particle. *Phys. Rev. C* **104**, 044003 (2021).
44. Krasznahorkay, A. J. et al. New anomaly observed in C12 supports the existence and the vector character of the hypothetical *X*17 boson. *Phys. Rev. C* **106**, L061601 (2022).
45. de Boer, F. W. N. et al. A deviation in internal pair conversion. *Phys. Lett. B* **388**, 235–240 (1996).
46. de Boer, F. W. N. et al. Further search for a neutral boson with a mass around 9-MeV/c^2. *J. Phys. G* **27**, L29 (2001).
47. Aleksejevs, A., Barkanova, S., Kolomensky, Y. G. & Sheff, B. A standard model explanation for the 'ATOMKI Anomaly'. Preprint at https://arxiv.org/abs/2102.01127 (2021).
48. Alves, D. S. M. et al. Shedding light on *X*17: community report. *Eur. Phys. J. C* **83**, 230 (2023).
49. Nomura, T. & Sanyal, P. Explaining Atomki anomaly and muon $g-2$ in $U(1)_X$ extended flavour violating two Higgs doublet model. *J. High Energy Phys.* **05**, 232 (2021).
50. Tien Du, P., Ai Viet, N. & Van Dat, N. Decay of neutron with participation of the light vector boson X17. *J. Phys. Conf. Ser.* **1506**, 012004 (2020).
51. Darmé, L., Mancini, M., Nardi, E. & Raggi, M. Resonant search for the *X*17 boson at PADME. *Phys. Rev. D* **106**, 115036 (2022).
52. Echenard, B., Essig, R. & Zhong, Y.-M. Projections for dark photon searches at Mu3e. *J. High Energy Phys.* **01**, 113 (2015).
53. Bastin, B. et al. Investigation of a light dark boson existence: the new JEDI project. *EPJ Web Conf.* **275**, 01012 (2023).
54. Aguilar, A. et al. Evidence for neutrino oscillations from the observation of $\overline{\nu}_e$ appearance in a $\overline{\nu}_e$ beam. *Phys. Rev. D* **64**, 112007 (2001).
55. Aguilar-Arevalo, A. A. et al. Significant excess of electron-like events in the MiniBooNE short-baseline neutrino experiment. *Phys. Rev. Lett.* **121**, 221801 (2018).
56. Aguilar-Arevalo, A. A. et al. Updated MiniBooNE neutrino oscillation results with increased data and new background studies. *Phys. Rev. D* **103**, 052002 (2021).
57. Brdar, V. & Kopp, J. Can standard model and experimental uncertainties resolve the MiniBooNE anomaly? *Phys. Rev. D* **105**, 115024 (2022).
58. Acciarri, R. et al. Design and construction of the MicroBooNE detector. *J. Instrum.* **12**, P02017 (2017).
59. Abratenko, P. et al. Search for an excess of electron neutrino interactions in MicroBooNE using multiple final-state topologies. *Phys. Rev. Lett.* **128**, 241801 (2022).
60. Aguilar-Arevalo, A. A. et al. MiniBooNE and MicroBooNE combined fit to a 3+1 sterile neutrino scenario. *Phys. Rev. Lett.* **129**, 201801 (2022).
61. Adamson, P. et al. Search for sterile neutrinos in MINOS and MINOS+ using a two-detector fit. *Phys. Rev. Lett.* **122**, 091803 (2019).
62. Aartsen, M. G. et al. eV-scale sterile neutrino search using eight years of atmospheric muon neutrino data from the IceCube Neutrino Observatory. *Phys. Rev. Lett.* **125**, 141801 (2020).
63. Dentler, M. et al. Updated global analysis of neutrino oscillations in the presence of eV-scale sterile neutrinos. *J. High Energy Phys.* **08**, 010 (2018).
64. Babu, K. S., Brdar, V., de Gouvêa, A. & Machado, P. A. N. Addressing the short-baseline neutrino anomalies with energy-dependent mixing parameters. *Phys. Rev. D* **107**, 015017 (2023).
65. Acero, M. A. et al. White paper on light sterile neutrino searches and related phenomenology. Preprint at https://arxiv.org/abs/2203.07323 (2022).
66. Declais, Y. et al. Search for neutrino oscillations at 15-meters, 40-meters, and 95-meters from a nuclear power reactor at Bugey. *Nucl. Phys. B* **434**, 503–534 (1995).
67. Apollonio, M. et al. Search for neutrino oscillations on a long baseline at the CHOOZ nuclear power station. *Eur. Phys. J. C* **27**, 331–374 (2003).
68. Mention, G. et al. The reactor antineutrino anomaly. *Phys. Rev. D* **83**, 073006 (2011).
69. Hampel, W. et al. Final results of the Cr-51 neutrino source experiments in GALLEX. *Phys. Lett. B* **420**, 114–126 (1998).
70. Kaether, F., Hampel, W., Heusser, G., Kiko, J. & Kirsten, T. Reanalysis of the GALLEX solar neutrino flux and source experiments. *Phys. Lett. B* **685**, 47–54 (2010).
71. Abdurashitov, J. N. et al. Measurement of the solar neutrino capture rate with gallium metal. III: results for the 2002–2007 data-taking period. *Phys. Rev. C* **80**, 015807 (2009).
72. Acero, M. A., Giunti, C. & Laveder, M. Limits on nu(e) and anti-nu(e) disappearance from gallium and reactor experiments. *Phys. Rev. D* **78**, 073009 (2008).
73. Giunti, C. & Laveder, M. Statistical significance of the gallium anomaly. *Phys. Rev. C* **83**, 065504 (2011).
74. Brdar, V., Gehrlein, J. & Kopp, J. Towards resolving the gallium anomaly. *J. High Energy Phys.* **05**, 143 (2023).
75. Giunti, C., Li, Y. F., Ternes, C. A. & Xin, Z. Reactor antineutrino anomaly in light of recent flux model refinements. *Phys. Lett. B* **829**, 137054 (2022).
76. Berryman, J. M., Coloma, P., Huber, P., Schwetz, T. & Zhou, A. Statistical significance of the sterile-neutrino hypothesis in the context of reactor and gallium data. *J. High Energy Phys.* **02**, 055 (2022).
77. Losada, M., Nir, Y., Perez, G., Savoray, I. & Shpilman, Y. Parametric resonance in neutrino oscillations induced by ultra-light dark matter and implications for KamLAND and JUNO. *J. High Energy Phys.* **03**, 032 (2023).
78. Barinov, V. V. et al. Search for electron-neutrino transitions to sterile states in the BEST experiment. *Phys. Rev. C* **105**, 065502 (2022).
79. Acciarri, R. et al. Long-Baseline Neutrino Facility (LBNF) and Deep Underground Neutrino Experiment (DUNE): conceptual design report, Vol. 2: the Physics Program for DUNE at LBNF (2015).
80. Fava, A. FNAL SBL Program Status. *PoS* **NuFACT2018**, 011 (2019).
81. Kobayashi, M. & Maskawa, T. CP violation in the renormalizable theory of weak interaction. *Prog. Theor. Phys.* **49**, 652–657 (1973).
82. Cabibbo, N. Unitary symmetry and leptonic decays. *Phys. Rev. Lett.* **10**, 531–533 (1963).
83. Czarnecki, A., Marciano, W. J. & Sirlin, A. Neutron lifetime and axial coupling connection. *Phys. Rev. Lett.* **120**, 202002 (2018).
84. Hardy, J. C. & Towner, I. S. Superallowed $0^+\to0^+$ nuclear β decays: 2020 critical survey, with implications for V_{ud} and CKM unitarity. *Phys. Rev. C* **102**, 045501 (2020).
85. Ambrosino, F. et al. Measurement of the absolute branching ratio for the $K^+\to\mu^+\nu(\gamma)$ decay with the KLOE detector. *Phys. Lett. B* **632**, 76–80 (2006).
86. Ambrosino, F. et al. Measurement of the charged kaon lifetime with the KLOE detector. *J. High Energy Phys.* **01**, 073 (2008).
87. Marciano, W. J. & Sirlin, A. Improved calculation of electroweak radiative corrections and the value of V_{ud}. *Phys. Rev. Lett.* **96**, 032002 (2006).
88. Seng, C.-Y., Gorchtein, M., Patel, H. H. & Ramsey-Musolf, M. J. Reduced hadronic uncertainty in the determination of V_{ud}. *Phys. Rev. Lett.* **121**, 241804 (2018).

89. Moulson, M. Experimental determination of V_{us} from kaon decays. *PoS* **CKM2016**, 033 (2017).
90. Seng, C.-Y., Galviz, D., Marciano, W. J. & Meißner, U.-G. Update on $|V_{us}|$ and $|V_{us}/V_{ud}|$ from semileptonic kaon and pion decays. *Phys. Rev. D* **105**, 013005 (2022).
91. Cirigliano, V., Crivellin, A., Hoferichter, M. & Moulson, M. Scrutinizing CKM unitarity with a new measurement of the $K_{\mu3}/K_{\mu2}$ branching fraction. *Phys. Lett. B* **838**, 137748 (2023).
92. Amhis, Y. S. et al. Averages of *b*-hadron, *c*-hadron, and *τ*-lepton properties as of 2021. *Phys. Rev. D* **107**, 052008 (2023).
93. Crivellin, A., Hoferichter, M. & Manzari, C. A. Fermi constant from muon decay versus electroweak fits and Cabibbo–Kobayashi–Maskawa Unitarity. *Phys. Rev. Lett.* **127**, 071801 (2021).
94. Capdevila, B., Crivellin, A., Manzari, C. A. & Montull, M. Explaining $b\to s\ell^+\ell^-$ and the Cabibbo angle anomaly with a vector triplet. *Phys. Rev. D* **103**, 015032 (2021).
95. Crivellin, A., Müller, D. & Schnell, L. Combined constraints on first generation leptoquarks. *Phys. Rev. D* **103**, 115023 (2021) (Addendum: *Phys. Rev. D* **104**, 055020 (2021)).
96. Crivellin, A., Kirk, F., Manzari, C. A. & Panizzi, L. Searching for lepton flavor universality violation and collider signals from a singly charged scalar singlet. *Phys. Rev. D* **103**, 073002 (2021).
97. Buras, A. J., Crivellin, A., Kirk, F., Manzari, C. A. & Montull, M. Global analysis of leptophilic Z' bosons. *J. High Energy Phys.* **06**, 068 (2021).
98. Coutinho, A. M., Crivellin, A. & Manzari, C. A. Global fit to modified neutrino couplings and the Cabibbo-angle anomaly. *Phys. Rev. Lett.* **125**, 071802 (2020).
99. Kirk, M. Cabibbo anomaly versus electroweak precision tests: an exploration of extensions of the standard model. *Phys. Rev. D* **103**, 035004 (2021).
100. Belfatto, B., Beradze, R. & Berezhiani, Z. The CKM unitarity problem: a trace of new physics at the TeV scale? *Eur. Phys. J. C* **80**, 149 (2020).
101. Branco, G. C., Penedo, J. T., Pereira, P. M. F., Rebelo, M. N. & Silva-Marcos, J. I. Addressing the CKM unitarity problem with a vector-like up quark. *J. High Energy Phys.* **07**, 099 (2021).
102. Belfatto, B. & Berezhiani, Z. Are the CKM anomalies induced by vector-like quarks? Limits from flavor changing and standard model precision tests. *J. High Energy Phys.* **10**, 079 (2021).
103. Crivellin, A., Kirk, M., Kitahara, T. & Mescia, F. Global fit of modified quark couplings to EW gauge bosons and vector-like quarks in light of the Cabibbo angle anomaly. *J. High Energy Phys.* **03**, 234 (2023).
104. Crivellin, A., Kirk, F., Manzari, C. A. & Montull, M. Global electroweak fit and vector-like leptons in light of the Cabibbo angle anomaly. *J. High Energy Phys.* **12**, 166 (2020).
105. Byrne, J. & Dawber, P. G. A revised value for the neutron lifetime measured using a Penning trap. *EPL* **33**, 187 (1996).
106. Yue, A. T. et al. Improved determination of the neutron lifetime. *Phys. Rev. Lett.* **111**, 222501 (2013).
107. Gonzalez, F. M. et al. Improved neutron lifetime measurement with UCNτ. *Phys. Rev. Lett.* **127**, 162501 (2021).
108. Fornal, B. & Grinstein, B. Dark matter interpretation of the neutron decay anomaly. *Phys. Rev. Lett.* **120**, 191801 (2018) (Erratum: *Phys. Rev. Lett.* **124**, 219901 (2020)).
109. Berezhiani, Z. Neutron lifetime puzzle and neutron–mirror neutron oscillation. *Eur. Phys. J. C* **79**, 484 (2019).
110. Brodeur, M. et al. Nuclear *β* decay as a probe for physics beyond the standard model. Preprint at https://arxiv.org/abs/2301.03975 (2023).
111. Altmannshofer, W. et al. PIONEER: studies of rare pion decays. Preprint at https://arxiv.org/abs/2203.01981 (2022).
112. Ayres, N. J. et al. Improved search for neutron to mirror-neutron oscillations in the presence of mirror magnetic fields with a dedicated apparatus at the PSI UCN source. *Symmetry* **14**, 503 (2022).
113. Bordone, M., Gubernari, N., Huber, T., Jung, M. & van Dyk, D. A puzzle in $\bar{B}^0_{(s)}\to D^{(*)+}_{(s)}\{\pi^-,K^-\}$ decays and extraction of the f_s/f_d fragmentation fraction. *Eur. Phys. J. C* **80**, 951 (2020).
114. Beneke, M., Buchalla, G., Neubert, M. & Sachrajda, C. T. QCD factorization in $B\to\pi K,\pi\pi$ decays and extraction of Wolfenstein parameters. *Nucl. Phys. B* **606**, 245–321 (2001).
115. Piscopo, M. L. & Rusov, A. V. Non-factorisable effects in the decays $\bar{B}^0_s\to D^+_s\pi^-$ and $\bar{B}^0_s\to D^+_s\pi^-$ from LCSR. *J. High Energy Phys.* **10**, 180 (2023).
116. Iguro, S. & Kitahara, T. Implications for new physics from a novel puzzle in $\bar{B}^0_{(s)}\to D^{(*)+}_{(s)}\{\pi^-,K^-\}$ decays. *Phys. Rev. D* **102**, 071701 (2020).
117. Bordone, M., Greljo, A. & Marzocca, D. Exploiting di-jet resonance searches for flavor physics. *J. High Energy Phys.* **08**, 036 (2021).
118. Aaij, R. et al. Evidence for CP violation in time-integrated $D^0\to h^-h^+$ decay rates. *Phys. Rev. Lett.* **108**, 111602 (2012).
119. Aaij, R. et al. Observation of *CP* violation in charm decays. *Phys. Rev. Lett.* **122**, 211803 (2019).
120. Chala, M., Lenz, A., Rusov, A. V. & Scholtz, J. ΔA_{CP} within the standard model and beyond. *J. High Energy Phys.* **07**, 161 (2019).
121. Aaij, R. et al. Measurement of the time-integrated *CP* asymmetry in $D^0\to K^-K^+$ decays. *Phys. Rev. Lett.* **131**, 091802 (2023).
122. Bause, R. et al. U-spin-CP anomaly in charm. *Phys. Rev. D* **108**, 035005 (2023).
123. Altmannshofer, W., Primulando, R., Yu, C.-T. & Yu, F. New physics models of direct CP violation in charm decays. *J. High Energy Phys.* **04**, 049 (2012).
124. Buras, A. J., Fleischer, R., Recksiegel, S. & Schwab, F. $B\to\pi\pi$, new physics in $B\to\pi K$ and implications for rare K and B decays. *Phys. Rev. Lett.* **92**, 101804 (2004).
125. Aaij, R. et al. Measurement of CP violation in the decay $B^+\to K^+\pi^0$. *Phys. Rev. Lett.* **126**, 091802 (2021).
126. Fleischer, R., Jaarsma, R. & Vos, K. K. Towards new frontiers with $B\to\pi K$ decays. *Phys. Lett. B* **785**, 525–529 (2018).
127. Aaij, R. et al. Measurement of *CP* asymmetries in two-body $B^0_{(s)}$-meson decays to charged pions and kaons. *Phys. Rev. D* **98**, 032004 (2018).
128. Algueró, M., Crivellin, A., Descotes-Genon, S., Matias, J. & Novoa-Brunet, M. A new *B*-flavour anomaly in $B_{d,s}\to K^{*0}\bar{K}^{*0}$: anatomy and interpretation. *J. High Energy Phys.* **04**, 066 (2021).
129. Calibbi, L., Crivellin, A., Kirk, F., Manzari, C. A. & Vernazza, L. Z' models with less-minimal flavour violation. *Phys. Rev. D* **101**, 095003 (2020).
130. Crivellin, A., Gross, C., Pokorski, S. & Vernazza, L. Correlating ϵ'/ϵ to hadronic *B* decays via $U(2)^3$ flavour symmetry. *Phys. Rev. D* **101**, 015022 (2020).
131. Buras, A. J. ε'/ε in the standard model and beyond: 2021. In *11th International Workshop on the CKM Unitarity Triangle*. Preprint at https://arxiv.org/abs/2203.12632 (2022).
132. Bhattacharya, B., Kumbhakar, S., London, D. & Payot, N. U-spin puzzle in B decays. *Phys. Rev. D* **107**, L011505 (2023).
133. Charles, J. et al. CP violation and the CKM matrix: assessing the impact of the asymmetric *B* factories. *Eur. Phys. J. C* **41**, 1–131 (2005).
134. Bona, M. et al. The 2004 UTfit collaboration report on the status of the unitarity triangle in the standard model. *J. High Energy Phys.* **07**, 028 (2005).
135. Gambino, P., Jung, M. & Schacht, S. The V_{cb} puzzle: an update. *Phys. Lett. B* **795**, 386–390 (2019).
136. Crivellin, A. & Pokorski, S. Can the differences in the determinations of V_{ub} and V_{cb} be explained by new physics? *Phys. Rev. Lett.* **114**, 011802 (2015).
137. Lees, J. P. et al. Evidence for an excess of $\bar{B}\to D^{(*)}\tau^-\bar{\nu}_\tau$ decays. *Phys. Rev. Lett.* **109**, 101802 (2012).
138. Lees, J. P. et al. Measurement of an excess of $\bar{B}\to D^{(*)}\tau^-\bar{\nu}_\tau$ decays and implications for charged Higgs bosons. *Phys. Rev. D* **88**, 072012 (2013).
139. Huschle, M. et al. Measurement of the branching ratio of $\bar{B}\to D^{(*)}\tau^-\bar{\nu}_\tau$ relative to $\bar{B}\to D^{(*)}\tau^-\bar{\nu}_\tau$ decays with hadronic tagging at Belle. *Phys. Rev. D* **92**, 072014 (2015).
140. Sato, Y. et al. Measurement of the branching ratio of $\bar{B}^0\to D^{*+}\tau^-\bar{\nu}_\tau$ relative to $\bar{B}^0\to D^{*+}\tau^-\bar{\nu}_\tau$ decays with a semileptonic tagging method. *Phys. Rev. D* **94**, 072007 (2016).
141. Hirose, S. et al. Measurement of the *τ* lepton polarization and $R(D^*)$ in the decay $\bar{B}\to D^*\tau^-\bar{\nu}_\tau$. *Phys. Rev. Lett.* **118**, 211801 (2017).
142. Hirose, S. et al. Measurement of the *τ* lepton polarization and $R(D^*)$ in the decay $\bar{B}\to D^*\tau^-\bar{\nu}_\tau$ with one-prong hadronic *τ* decays at Belle. *Phys. Rev. D* **97**, 012004 (2018).
143. Caria, G. et al. Measurement of $\mathcal{R}(D)$ and $\mathcal{R}(D)$ with a semileptonic tagging method. *Phys. Rev. Lett.* **124**, 161803 (2020).
144. Aaij, R. et al. Measurement of the ratio of branching fractions $\mathcal{B}(\bar{B}^0\to D^{*+}\tau^-\bar{\nu}_\tau)/\mathcal{B}(\bar{B}^0\to D^{*+}\mu^-\bar{\nu}_\mu)$. *Phys. Rev. Lett.* **115**, 111803 (2015) (Erratum: *Phys. Rev. Lett.* **115**, 159901 (2015)).
145. Aaij, R. et al. Measurement of the ratio of the $B^0\to D^{*-}\tau^+\nu_\tau$ and $B^0\to D^{*-}\mu^+\nu_\mu$ branching fractions using three-prong *τ*-lepton decays. *Phys. Rev. Lett.* **120**, 171802 (2018).
146. Aaij, R. et al. Test of lepton flavor universality by the measurement of the $B^0\to D^{*-}\tau^+\nu_\tau$ branching fraction using three-prong *τ* decays. *Phys. Rev. D* **97**, 072013 (2018).
147. Crivellin, A., Greub, C. & Kokulu, A. Explaining $B\to D\tau\nu$, $B\to D^*\tau\nu$ and $B\to\tau\nu$ in a 2HDM of type III. *Phys. Rev. D* **86**, 054014 (2012).
148. Fajfer, S., Kamenik, J. F., Nisandzic, I. & Zupan, J. Implications of lepton flavor universality violations in B decays. *Phys. Rev. Lett.* **109**, 161801 (2012).
149. Celis, A., Jung, M., Li, X.-Q. & Pich, A. Sensitivity to charged scalars in $\boldsymbol{B\to D^{(*)}\tau\nu_\tau}$ and $\boldsymbol{B\to\tau\nu_\tau}$ decays. *J. High Energy Phys.* **01**, 054 (2013).
150. Bhattacharya, B., Datta, A., London, D. & Shivashankara, S. Simultaneous explanation of the R_K and $R(D^{(*)})$ puzzles. *Phys. Lett. B* **742**, 370–374 (2015).
151. Sakaki, Y., Tanaka, M., Tayduganov, A. & Watanabe, R. Testing leptoquark models in $\bar{B}\to D^{(*)}\tau\bar{\nu}$. *Phys. Rev. D* **88**, 094012 (2013).
152. Freytsis, M., Ligeti, Z. & Ruderman, J. T. Flavor models for $\bar{B}\to D^{(*)}\tau\bar{\nu}$. *Phys. Rev. D* **92**, 054018 (2015).
153. Fajfer, S. & Košnik, N. Vector leptoquark resolution of R_K and $R_{D^{(*)}}$ puzzles. *Phys. Lett. B* **755**, 270–274 (2016).
154. Iguro, S. Revival of H^- interpretation of $R(D^{(*)})$ anomaly and closing low mass window. *Phys. Rev. D* **105**, 095011 (2022).
155. Blanke, M., Iguro, S. & Zhang, H. Towards ruling out the charged Higgs interpretation of the $R_{D^{(*)}}$ anomaly. *J. High Energy Phys.* **06**, 043 (2022).
156. Greljo, A., Isidori, G. & Marzocca, D. On the breaking of lepton flavor universality in *B* decays. *J. High Energy Phys.* **07**, 142 (2015).
157. Calibbi, L., Crivellin, A. & Ota, T. Effective field theory approach to Springer InlineMath and $B\to D^{(*)}\tau\nu$ with third generation couplings. *Phys. Rev. Lett.* **115**, 181801 (2015).
158. Barbieri, R., Murphy, C. W. & Senia, F. *β*-decay anomalies in a composite leptoquark model. *Eur. Phys. J. C* **77**, 8 (2017).
159. Di Luzio, L., Greljo, A. & Nardecchia, M. Gauge leptoquark as the origin of *B*-physics anomalies. *Phys. Rev. D* **96**, 115011 (2017).
160. Calibbi, L., Crivellin, A. & Li, T. Model of vector leptoquarks in view of the *B*-physics anomalies. *Phys. Rev. D* **98**, 115002 (2018).
161. Bordone, M., Cornella, C., Fuentes-Martin, J. & Isidori, G. A three-site gauge model for flavor hierarchies and flavor anomalies. *Phys. Lett. B* **779**, 317–323 (2018).
162. Blanke, M. & Crivellin, A. *B* meson anomalies in a Pati–Salam model within the Randall–Sundrum background. *Phys. Rev. Lett.* **121**, 011801 (2018).
163. King, S. F. Twin Pati–Salam theory of flavour with a TeV scale vector leptoquark. *J. High Energy Phys.* **11**, 161 (2021).
164. Crivellin, A., Müller, D. & Ota, T. Simultaneous explanation of $R(D^{()})$ and $b\to s\mu^+\mu$: the last scalar leptoquarks standing. *J. High Energy Phys.* **09**, 040 (2017).

165. Crivellin, A., Müller, D. & Saturnino, F. Flavor phenomenology of the leptoquark singlet-triplet model. *J. High Energy Phys.* **06**, 020 (2020).
166. Gherardi, V., Marzocca, D. & Venturini, E. Low-energy phenomenology of scalar leptoquarks at one-loop accuracy. *J. High Energy Phys.* **01**, 138 (2021).
167. Bainbridge, R. Recording and reconstructing 10 billion unbiased b hadron decays in CMS. *EPJ Web Conf.* **245**, 01025 (2020).
168. Aaij, R. et al. Tests of lepton universality using $B^0 \to K^0_S \ell^+\ell^-$ and $B^+ \to K^{*+}\ell^+\ell^-$ decays. *Phys. Rev. Lett.* **128**, 191802 (2022).
169. Aaij, R. et al. Test of lepton universality in $b \to s\ell^+\ell^-$ decays. *Phys. Rev. Lett.* **131**, 051803 (2023).
170. ATLAS, CMS & LHCb Collaborations. Combination of the ATLAS, CMS and LHCb results on the $B^0_{(s)} \to \mu^+\mu^-$ decays. Report No. CMS-PAS-BPH-20-003 (CERN Document Server, 2020).
171. Tumasyan, A. et al. Measurement of the $B^0_s \to \mu^+\mu^-$ decay properties and search for the $B^0 \to \mu^+\mu^-$ decay in proton–proton collisions at $B^0_s \to \mu^+\mu^-$ = 13 TeV. *Phys. Lett. B* **842**, 137955 (2023).
172. Hermann, T., Misiak, M. & Steinhauser, M. Three-loop QCD corrections to $B_s \to \mu^+\mu^-$. *J. High Energy Phys.* **12**, 097 (2013).
173. Beneke, M., Bobeth, C. & Szafron, R. Enhanced electromagnetic correction to the rare *B*-meson decay $B_{s,d} \to \mu^+\mu^-$. *Phys. Rev. Lett.* **120**, 011801 (2018).
174. Descotes-Genon, S., Matias, J., Ramon, M. & Virto, J. Implications from clean observables for the binned analysis of $B \to K^*\mu^+\mu^-$ at large recoil. *J. High Energy Phys.* **01**, 048 (2013).
175. Aaij, R. et al. Measurement of *CP*-averaged observables in the $B^0 \to K^{*0}\mu^+\mu^-$ decay. *Phys. Rev. Lett.* **125**, 011802 (2020).
176. Aaij, R. et al. Differential branching fractions and isospin asymmetries of $B \to K^{(*)}\mu^+\mu^-$ decays. *J. High Energy Phys.* **06**, 133 (2014).
177. Parrott, W. G., Bouchard, C. & Davies, C. T. H. Standard model predictions for $B \to K\ell^+\ell^-$, $B \to K\ell_1^-\ell_2^+$ and $B \to K\nu\nu$ using form factors from Nf=2+1+1 lattice QCD. *Phys. Rev. D* **107**, 014511 (2023) (Erratum: *Phys. Rev. D* **107**, 119903 (2023)).
178. Aaij, R. et al. Branching fraction measurements of the rare $B^0_s \to \phi\mu^+\mu^-$ and $B^0_s \to \phi\mu^+\mu^-$ -decays. *Phys. Rev. Lett.* **127**, 151801 (2021).
179. Gubernari, N., Reboud, M., van Dyk, D. & Virto, J. Improved theory predictions and global analysis of exclusive $b \to s\mu^+\mu^-$ processes. *J. High Energy Phys.* **09**, 133 (2022).
180. Isidori, G., Polonsky, Z. & Tinari, A. Semi-inclusive $b \to s\bar{\ell}\ell$ transitions at high q^2. *Phys. Rev. D* **108**, 093008 (2023).
181. Buras, A. J. Standard model predictions for rare *K* and *B* decays without new physics infection. *Eur. Phys. J. C* **83**, 66 (2023).
182. Ciuchini, M. et al. Constraints on lepton universality violation from rare *B* decays. *Phys. Rev. D* **107**, 055036 (2023).
183. Algueró, M. et al. To (b)e or not to (b)e: no electrons at LHCb. *Eur. Phys. J. C* **83**, 648 (2023).
184. Belle II Collaboration. Evidence for $B^+ \to K^+\nu\bar{\nu}$ decays Preprint at https://arxiv.org/abs/2311.14647 (2023).
185. Algueró, M., Matias, J., Capdevila, B. & Crivellin, A. Disentangling lepton flavor universal and lepton flavor universality violating effects in $b \to s\ell^+\ell^-$ transitions. *Phys. Rev. D* **105**, 113007 (2022).
186. Buras, A. J. & Girrbach, J. Left-handed *Z*′ and *Z* FCNC quark couplings facing new $b \to s\mu^+\mu^-$ data. *J. High Energy Phys.* **12**, 009 (2013).
187. Gauld, R., Goertz, F. & Haisch, U. On minimal *Z*′ explanations of the $B \to K^*\mu^+\mu^-$ anomaly. *Phys. Rev. D* **89**, 015005 (2014).
188. Di Luzio, L., Kirk, M. & Lenz, A. Updated B_s-mixing constraints on new physics models for $b \to s\ell^+\ell^-$ anomalies. *Phys. Rev. D* **97**, 095035 (2018).
189. Allanach, B., Queiroz, F. S., Strumia, A. & Sun, S. *Z*′ models for the LHCb and *g*−2 muon anomalies. *Phys. Rev. D* **93**, 055045 (2016) (Erratum: *Phys. Rev. D* **95**, 119902 (2017)).
190. LEP Collaborations, LEP Electroweak Working Group, SLD Electroweak & Heavy Flavour Groups. A combination of preliminary electroweak measurements and constraints on the standard model. Preprint at https://arxiv.org/abs/hep-ex/0312023 (2004).
191. Crivellin, A. et al. Lepton-flavour violating *B* decays in generic *Z*′ models. *Phys. Rev. D* **92**, 054013 (2015).
192. Crivellin, A., D'Ambrosio, G. & Heeck, J. Addressing the LHC flavor anomalies with horizontal gauge symmetries. *Phys. Rev. D* **91**, 075006 (2015).
193. Bobeth, C., Haisch, U., Lenz, A., Pecjak, B. & Tetlalmatzi-Xolocotzi, G. On new physics in $\Delta\Gamma_d$. *J. High Energy Phys.* **06**, 040 (2014).
194. Crivellin, A., Fuks, B. & Schnell, L. Explaining the hints for lepton flavour universality violation with three S_2 leptoquark generations. *J. High Energy Phys.* **06**, 169 (2022).
195. Crivellin, A., Greub, C., Müller, D. & Saturnino, F. Importance of loop effects in explaining the accumulated evidence for new physics in *B* decays with a vector leptoquark. *Phys. Rev. Lett.* **122**, 011805 (2019).
196. Crivellin, A., Kokulu, A. & Greub, C. Flavor-phenomenology of two-Higgs-doublet models with generic Yukawa structure. *Phys. Rev. D* **87**, 094031 (2013).
197. Crivellin, A., Müller, D. & Wiegand, C. $b \to s\ell^+\ell^-$ transitions in two-Higgs-doublet models. *J. High Energy Phys.* **06**, 119 (2019).
198. Iguro, S. Conclusive probe of the charged Higgs solution of Springer InlineMath and $R(D^{(*)})$ discrepancies. *Phys. Rev. D* **107**, 095004 (2023).
199. Crivellin, A. & Kirk, M. Diquark explanation of $b \to s\ell^+\ell^-$. *Phys. Rev. D* **108**, L111701 (2023).
200. Gubernari, N., Reboud, M., van Dyk, D. & Virto, J. Dispersive analysis of $B \to K^{(*)}$ and $B_s \to \phi$ form factors. *J. High Energ. Phys.* **2023**, 153 (2023).
201. Aaltonen, T. et al. High-precision measurement of the *W* boson mass with the CDF II detector. *Science* **376**, 170–176 (2022).
202. Aaboud, M. et al. Measurement of the *W*-boson mass in pp collisions at $\sqrt{s}$ = 7 TeV with the ATLAS detector. *Eur. Phys. J. C* **78**, 110 (2018). (Erratum: *Eur. Phys. J. C* **78**, 898 (2018)).
203. Chatrchyan, S. et al. Measurement of the weak mixing angle with the Drell–Yan process in proton–proton collisions at the LHC. *Phys. Rev. D* **84**, 112002 (2011).
204. Aaij, R. et al. Measurement of the forward–backward asymmetry in $Z/\gamma^* \to \mu^+\mu^-$ decays and determination of the effective weak mixing angle. *J. High Energy Phys.* **11**, 190 (2015).
205. Aaij, R. et al. Measurement of the *W* boson mass. *J. High Energy Phys.* **01**, 036 (2022).
206. Schael, S. et al. Electroweak measurements in electron–positron collisions at *W*-boson-pair energies at LEP. *Phys. Rep.* **532**, 119–244 (2013).
207. de Blas, J., Pierini, M., Reina, L. & Silvestrini, L. Impact of the recent measurements of the top-quark and *W*-boson masses on electroweak precision fits. *Phys. Rev. Lett.* **129**, 271801 (2022).
208. ATLAS Collaboration. Improved *W* boson mass measurement using 7 TeV proton–proton collisions with the ATLAS detector. Report No. ATLAS-CONF-2023-004 (CERN Document Server, 2023).
209. Schael, S. et al. Precision electroweak measurements on the *Z* resonance. *Phys. Rep.* **427**, 257–454 (2006).
210. Konetschny, W. & Kummer, W. Nonconservation of total lepton number with scalar bosons. *Phys. Lett. B* **70**, 433–435 (1977).
211. Algueró, M., Matias, J., Crivellin, A. & Manzari, C. A. Unified explanation of the anomalies in semileptonic *B* decays and the W mass. *Phys. Rev. D* **106**, 033005 (2022).
212. Crivellin, A., Kirk, M., Kitahara, T. & Mescia, F. Large $t \to cZ$ as a sign of vectorlike quarks in light of the *W* mass. *Phys. Rev. D* **106**, L031704 (2022).
213. Crivellin, A., Müller, D. & Saturnino, F. Leptoquarks in oblique corrections and Higgs signal strength: status and prospects. *J. High Energy Phys.* **11**, 094 (2020).
214. Strumia, A. Interpreting electroweak precision data including the *W*-mass CDF anomaly. *J. High Energy Phys.* **08**, 248 (2022).
215. Baer, H. et al. The International Linear Collider Technical Design Report — Vol. 2: Physics. Preprint at https://arxiv.org/abs/1306.6352 (2013).
216. Linssen, L., Miyamoto, A., Stanitzki, M. & Weerts, H. (eds) Physics and Detectors at CLIC: CLIC Conceptual Design Report. CERN Yellow Report CERN-2012-003 (CERN Document Server, 2012).
217. Charles, T. K. et al. The Compact Linear Collider (CLIC) — 2018 Summary Report 2/2018. Preprint at https://arxiv.org/abs/1812.06018 (2018).
218. Abada, A. et al. FCC-ee: the lepton collider: future circular collider conceptual design report volume 2. *Eur. Phys. J. ST* **228**, 261–623 (2019).
219. Abada, A. et al. FCC physics opportunities: future circular collider conceptual design report volume 1. *Eur. Phys. J. C* **79**, 474 (2019).
220. Dong, M. et al. CEPC conceptual design report: volume 2 — physics & detector. Preprint at https://arxiv.org/abs/1811.10545 (2018).
221. An, F. et al. Precision Higgs physics at the CEPC. *Chin. Phys. C* **43**, 043002 (2019).
222. Fischer, O. et al. Unveiling hidden physics at the LHC. *Eur. Phys. J. C* **82**, 665 (2022).
223. von Buddenbrock, S. et al. Phenomenological signatures of additional scalar bosons at the LHC. *Eur. Phys. J. C* **76**, 580 (2016).
224. von Buddenbrock, S. et al. Multi-lepton signatures of additional scalar bosons beyond the standard model at the LHC. *J. Phys. G* **45**, 115003 (2018).
225. Buddenbrock, S. et al. The emergence of multi-lepton anomalies at the LHC and their compatibility with new physics at the EW scale. *J. High Energy Phys.* **10**, 157 (2019).
226. Hernandez, Y. et al. The anomalous production of multi-lepton and its impact on the measurement of *Wh* production at the LHC. *Eur. Phys. J. C* **81**, 365 (2021).
227. von Buddenbrock, S., Ruiz, R. & Mellado, B. Anatomy of inclusive $t\bar{t}W$ production at hadron colliders. *Phys. Lett. B* **811**, 135964 (2020).
228. Banik, S., Coloretti, G., Crivellin, A. & Mellado, B. Uncovering new Higgses in the LHC analyses of Differential $t\bar{t}$ cross sections (2023). Preprint at https://arxiv.org/abs/2308.07953 (2023).
229. Aad, G. et al. Inclusive and differential cross-sections for dilepton $t\bar{t}$ production measured in $t\bar{t}$ = 13 TeV pp collisions with the ATLAS detector. *J. High Energy Phys.* **07**, 141 (2023).
230. Czakon, M., Mitov, A. & Poncelet, R. NNLO QCD corrections to leptonic observables in top-quark pair production and decay. *J. High Energy Phys.* **05**, 212 (2021).
231. Gehrmann, T. et al. W^+W^- production at hadron colliders in next to next to leading order QCD. *Phys. Rev. Lett.* **113**, 212001 (2014).
232. Grazzini, M., Kallweit, S., Pozzorini, S., Rathlev, D. & Wiesemann, M. W^+W production at the LHC: fiducial cross sections and distributions in NNLO QCD. *J. High Energy Phys.* **08**, 140 (2016).
233. Hamilton, K., Melia, T., Monni, P. F., Re, E. & Zanderighi, G. Merging *WW* and *WW*+jet with MINLO. *J. High Energy Phys.* **09**, 057 (2016).
234. Re, E., Wiesemann, M. & Zanderighi, G. NNLOPS accurate predictions for W^+W^- production. *J. High Energy Phys.* **12**, 121 (2018).
235. Caola, F., Melnikov, K., Röntsch, R. & Tancredi, L. QCD corrections to W^+W^- production through gluon fusion. *Phys. Lett. B* **754**, 275–280 (2016).
236. Grazzini, M., Kallweit, S., Rathlev, D. & Wiesemann, M. $W^{\pm}Z$ production at the LHC: fiducial cross sections and distributions in NNLO QCD. *J. High Energy Phys.* **05**, 139 (2017).
237. Brein, O., Djouadi, A. & Harlander, R. NNLO QCD corrections to the Higgs-strahlung processes at hadron colliders. *Phys. Lett. B* **579**, 149–156 (2004).
238. Ferrera, G., Grazzini, M. & Tramontano, F. Associated WH production at hadron colliders: a fully exclusive QCD calculation at NNLO. *Phys. Rev. Lett.* **107**, 152003 (2011).
239. Campbell, J. M., Ellis, R. K. & Williams, C. Associated production of a Higgs boson at NNLO. *J. High Energy Phys.* **06**, 179 (2016).

240. Buonocore, L. et al. Precise predictions for the associated production of a *W* boson with a top-antitop quark pair at the LHC. *Phys. Rev. Lett.* **131**, 231901 (2023).
241. Ciccolini, M. L., Dittmaier, S. & Kramer, M. Electroweak radiative corrections to associated *WH* and *ZH* production at hadron colliders. *Phys. Rev. D* **68**, 073003 (2003).
242. Denner, A., Dittmaier, S., Kallweit, S. & Muck, A. Electroweak corrections to Higgs-strahlung off *W*/*Z* bosons at the Tevatron and the LHC with HAWK. *J. High Energy Phys.* **03**, 075 (2012).
243. Denner, A. & Pellen, M. NLO electroweak corrections to off-shell top–antitop production with leptonic decays at the LHC. *J. High Energy Phys.* **08**, 155 (2016).
244. Biedermann, B. et al. Next-to-leading-order electroweak corrections to $pp \to W^+W^- \to 4$ leptons at the LHC. *J. High Energy Phys.* **06**, 065 (2016).
245. Dittmaier, S., Knippen, G. & Schwan, C. Next-to-leading-order QCD and electroweak corrections to triple-*W* production with leptonic decays at the LHC. *J. High Energy Phys.* **02**, 003 (2020).
246. Sirunyan, A. M. et al. Search for heavy Higgs bosons decaying to a top quark pair in proton–proton collisions at $\sqrt{s} = 13$ TeV. *J. High Energy Phys.* **04**, 171 (2020) (Erratum: *J. High Energy Phys.* **03**, 187 (2022)).
247. Coloretti, G., Crivellin, A., Bhattacharya, S. & Mellado, B. Searching for low-mass resonances decaying into *W* bosons. *Phys. Rev. D* **108**, 035026 (2023).
248. Ježo, T., Lindert, J. M. & Pozzorini, S. Resonance-aware NLOPS matching for off-shell $t\bar{t} + tW$ production with semileptonic decays. *J. High Energy Phys.* **10**, 008 (2023).
249. CMS Collaboration. Search for a standard model-like Higgs boson in the mass range between 70 and 110 GeV in the diphoton final state in proton–proton collisions at $\sqrt{s} = 13$ TeV. Report No. CMS-PAS-HIG-20-002 (CERN Document Server, 2023).
250. ATLAS Collaboration. Search for diphoton resonances in the 66 to 110 GeV mass range using 140 fb^{-1} of 13 TeV *pp* collisions collected with the ATLAS detector. Report No. ATLAS-CONF-2023-035 (CERN Document Server, 2023).
251. Aad, G. et al. Search for dark matter in events with missing transverse momentum and a Higgs boson decaying into two photons in pp collisions at $\sqrt{s} = 13$ TeV with the ATLAS detector. *J. High Energy Phys.* **10**, 013 (2021).
252. Sirunyan, A. M. et al. Measurements of properties of the Higgs boson decaying into the four-lepton final state in pp collisions at $\sqrt{s} = 13$ TeV. *J. High Energy Phys.* **11**, 047 (2017).
253. Aad, G. et al. Search for resonances decaying into photon pairs in 139 fb^{-1} of *pp* collisions at $\sqrt{s}$=13 TeV with the ATLAS detector. *Phys. Lett. B* **822**, 136651 (2021).
254. CMS Collaboration. Searches for additional Higgs bosons and vector leptoquarks in $\tau\tau$ final states in proton–proton collisions at $\sqrt{s} = 13$ TeV. *J. High Energy Phys.* **2023**, 73 (2023).
255. Aad, G. et al. Measurements of Higgs boson production cross-sections in the $H \to \tau^+\tau^-$ decay channel in pp collisions at $\sqrt{s} = 13$ TeV with the ATLAS detector. *J. High Energy Phys.* **08**, 175 (2022).
256. Barate, R. et al. Search for the standard model Higgs boson at LEP. *Phys. Lett. B* **565**, 61–75 (2003).
257. Aad, G. et al. Model-independent search for the presence of new physics in events including $H \to \gamma\gamma$ with $\sqrt{s} = 13$ TeV pp data recorded by the ATLAS detector at the LHC. *J. High Energy Phys.* **07**, 176 (2023).
258. Bhattacharya, S. et al. Growing excesses of new scalars at the electroweak scale. Preprint at https://arxiv.org/abs/2306.17209 (2023).
259. Crivellin, A. et al. Accumulating evidence for the associated production of a new Higgs boson at the LHC. *Phys. Rev. D* **108**, 115031 (2023).
260. Consoli, M., Cosmai, L. & Fabbri, F. Second resonance of the Higgs field: more signals from the LHC experiments. Preprint at https://arxiv.org/abs/2208.00920 (2022).
261. Aad, G. et al. Search for heavy resonances decaying into a pair of Z bosons in the $\ell^+\ell^-\ell'^+\ell'^-$ and $\ell^+\ell^-\ell'^+\ell'^-$ final states using 139 fb^{-1} of proton–proton collisions at $\ell^+\ell^-\ell'^+\ell'^-$ TeV with the ATLAS detector. *Eur. Phys. J. C* **81**, 332 (2021).
262. CMS Collaboration. Search for a new resonance decaying to two spin-0 bosons in a final state with two photons and two bottom quarks in proton–proton collisions at $\sqrt{s} = 13$ TeV. Preprint at https://doi.org/10.48550/arXiv.2310.01643 (2023).
263. CMS Collaboration. Search for high mass resonances decaying into W^+W^- in the dileptonic final state with 138 fb^{-1} of proton–proton collisions at $\sqrt{s} = 13$ TeV. Report No. CMS-PAS-HIG-20-016 (CERN Document Server, 2022).
264. Tumasyan, A. et al. Search for a heavy Higgs boson decaying into two lighter Higgs bosons in the $\tau\tau bb$ final state at 13 TeV. *J. High Energy Phys.* **11**, 057 (2021).
265. Le Yaouanc, A. & Richard, F. As a consequence of $H(650) \to W^+W^-/ZZ$, one predicts $H^{++} \to W^+W^+$ and $H^+ \to ZW^+$, as indicated by LHC data. In *2nd ECFA Workshop on e+e- Higgs/EW/Top Factories*. Preprint at https://arxiv.org/abs/2308.12180 (2023).
266. Haisch, U. & Malinauskas, A. Let there be light from a second light Higgs doublet. *J. High Energy Phys.* **03**, 135 (2018).
267. Ashanujjaman, S. et al. $SU(2)_L$ triplet scalar as the origin of the 95 GeV excess? *Phys. Rev. D* **108**, L091704 (2023).
268. Biekötter, T., Heinemeyer, S. & Weiglein, G. Excesses in the low-mass Higgs-boson search and the *W*-boson mass measurement. *Eur. Phys. J. C* **83**, 450 (2023).
269. Banik, S., Crivellin, A., Iguro, S. & Kitahara, T. Asymmetric di-Higgs signals of the next-to-minimal 2HDM with a *U*(1) symmetry. *Phys. Rev. D* **108**, 075011 (2023).
270. Georgi, H. & Machacek, M. Doubly charged HIGGS bosons. *Nucl. Phys. B* **262**, 463–477 (1985).
271. Kundu, A., Le Yaouanc, A., Mondal, P. & Richard, F. Searches for scalars at LHC and interpretation of the findings. In *2022 ECFA Workshop on e+e- Higgs/EW/Top factories*. Preprint at https://arxiv.org/abs/2211.11723 (2022).
272. Consoli, M. & Cosmai, L. A resonance of the Higgs field at 700 GeV and a new phenomenology. Preprint at https://arxiv.org/abs/2007.10837 (2020).
273. Cid Vidal, X. et al. Report from Working Group 3: beyond the Standard Model physics at the HL-LHC and HE-LHC. *CERN Yellow Rep. Monogr.* **7**, 585–865 (2019).
274. Aaboud, M. et al. Search for low-mass dijet resonances using trigger-level jets with the ATLAS detector in *pp* collisions at $\sqrt{s} = 13$ TeV. *Phys. Rev. Lett.* **121**, 081801 (2018).
275. Tumasyan, A. et al. Search for resonant and nonresonant production of pairs of dijet resonances in proton–proton collisions at $\sqrt{s} = 13$ TeV. *J. High Energy Phys.* **07**, 161 (2023).
276. Crivellin, A., Manzari, C. A., Mellado, B. & Dahbi, S.-E. Consistency and interpretation of the LHC dijet excesses. *Phys. Rev. D* **107**, 054045 (2023).
277. Aad, G. et al. Pursuit of paired dijet resonances in the Run 2 dataset with ATLAS. *Phys. Rev. D* **108**, 112005 (2023).
278. Aad, G. et al. Search for vector–boson resonances decaying into a top quark and a bottom quark using *pp* collisions at $\sqrt{s} = 13$ TeV with the ATLAS detector. *J. High Energ. Phys.* **2023**, 73 (2023).
279. Sirunyan, A. M. et al. Search for resonant and nonresonant new phenomena in high-mass dilepton final states at $\sqrt{s} = 13$ TeV. *J. High Energy Phys.* **07**, 208 (2021).
280. Aad, G. et al. Search for new non-resonant phenomena in high-mass dilepton final states with the ATLAS detector. *J. High Energy Phys.* **11**, 005 (2020) (Erratum: *J. High Energy Phys.* **04**, 142 (2021)).
281. Greljo, A. & Marzocca, D. High-p_T dilepton tails and flavor physics. *Eur. Phys. J. C* **77**, 548 (2017).
282. Crivellin, A., Manzari, C. A. & Montull, M. Correlating nonresonant di-electron searches at the LHC to the Cabibbo-angle anomaly and lepton flavor universality violation. *Phys. Rev. D* **104**, 115016 (2021).
283. Crivellin, A., Hoferichter, M., Kirk, M., Manzari, C. A. & Schnell, L. First-generation new physics in simplified models: from low-energy parity violation to the LHC. *J. High Energy Phys.* **10**, 221 (2021).
284. Fernández Navarro, M. & King, S. F. B-anomalies in a twin Pati–Salam theory of flavour including the 2022 LHCb $R_{K^{(*)}}$ analysis. *J. High Energy Phys.* **02**, 188 (2023).
285. Aebischer, J., Isidori, G., Pesut, M., Stefanek, B. A. & Wilsch, F. Confronting the vector leptoquark hypothesis with new low- and high-energy data. *Eur. Phys. J. C* **83**, 153 (2023).
286. Aaboud, M. et al. Measurement of fiducial and differential W^+W^- production cross-sections at $\sqrt{s} = 13$ TeV with the ATLAS detector. *Eur. Phys. J. C* **79**, 884 (2019).
287. Aad, G. et al. Observation of four-top-quark production in the multilepton final state with the ATLAS detector. *Eur. Phys. J. C* **83**, 496 (2023).
288. Hayrapetyan, A. et al. Observation of four top quark production in proton–proton collisions at s=13 TeV. *Phys. Lett. B* **847**, 138290 (2023).
289. CMS Collaboration. Measurement of Higgs boson production in association with a W or Z boson in the $H \to WW$ decay channel. Report No. CMS-PAS-HIG-19-017 (CERN Document Server, 2021).
290. Aad, G. et al. Observation of *WWW* production in *pp* collisions at $\sqrt{s}$ =13 TeV with the ATLAS detector. *Phys. Rev. Lett.* **129**, 061803 (2022).
291. Tumasyan, A. et al. Measurements of the Higgs boson production cross section and couplings in the W boson pair decay channel in proton–proton collisions at $\sqrt{s} = 13$ TeV. *Eur. Phys. J. C* **83**, 667 (2023).
292. Buchmuller, W., Ruckl, R. & Wyler, D. Leptoquarks in lepton–quark collisions. *Phys. Lett. B* **191**, 442–448 (1987) (Erratum: *Phys. Lett. B* **448**, 320–320 (1999)).
293. Doršner, I., Fajfer, S., Greljo, A., Kamenik, J. F. & Košnik, N. Physics of leptoquarks in precision experiments and at particle colliders. *Phys. Rep.* **641**, 1–68 (2016).
294. Pati, J. C. & Salam, A. Lepton number as the fourth color. *Phys. Rev. D* **10**, 275–289 (1974) (Erratum: *Phys. Rev. D* **11**, 703–703 (1975)).
295. Georgi, H. & Glashow, S. L. Unity of all elementary particle forces. *Phys. Rev. Lett.* **32**, 438–441 (1974).
296. Barbier, R. et al. R-parity violating supersymmetry. *Phys. Rep.* **420**, 1–202 (2005).
297. Hewett, J. L. & Rizzo, T. G. Low-energy phenomenology of superstring inspired *E*(6) models. *Phys. Rep.* **183**, 193 (1989).
298. Weinberg, S. Elementary particle theory of composite particles. *Phys. Rev.* **130**, 776–783 (1963).
299. Randall, L. & Sundrum, R. A large mass hierarchy from a small extra dimension. *Phys. Rev. Lett.* **83**, 3370–3373 (1999).
300. Froggatt, C. D. & Nielsen, H. B. Hierarchy of quark masses, Cabibbo angles and *CP* violation. *Nucl. Phys. B* **147**, 277–298 (1979).
301. Mohapatra, R. N. & Pati, J. C. A natural left-right symmetry. *Phys. Rev. D* **11**, 2558 (1975).
302. Langacker, P. Grand unified theories and proton decay. *Phys. Rep.* **72**, 185 (1981).
303. Antoniadis, I. A possible new dimension at a few TeV. *Phys. Lett. B* **246**, 377–384 (1990).
304. Haber, H. E. & Kane, G. L. The search for supersymmetry: probing physics beyond the standard model. *Phys. Rep.* **117**, 75–263 (1985).
305. Minkowski, P. $\mu \to e\gamma$ at a rate of one out of 10^9 muon decays? *Phys. Lett. B* **67**, 421–428 (1977).
306. Lee, B. W. & Shrock, R. E. Natural suppression of symmetry violation in gauge theories: muon–lepton and electron lepton number nonconservation. *Phys. Rev. D* **16**, 1444 (1977).
307. Foot, R., Lew, H., He, X. G. & Joshi, G. C. Seesaw neutrino masses induced by a triplet of leptons. *Z. Phys. C* **44**, 441 (1989).
308. Chanowitz, M. S. & Golden, M. Higgs boson triplets with $M_W = M_Z \cos\theta\omega$. *Phys. Lett. B* **165**, 105–108 (1985).
309. Branco, G. C. et al. Theory and phenomenology of two-Higgs-doublet models. *Phys. Rep.* **516**, 1–102 (2012).

Acknowledgements

The work of A.C. is supported by a professorship grant from the Swiss National Science Foundation (No. PP00P2_211002). B.M. gratefully acknowledges the South African Department of Science and Innovation through the SA-CERN programme, the National Research Foundation and the Research Office of the University of the Witwatersrand for various forms of support. The authors thank W. Murray for pointing to excess in the *Zhh* final state and L. Donaldson for assistance with the prospects of investigating the *X*17 anomaly.

Author contributions

The main part of the writing was done by A.C.; B.M. contributed to sections on the definition of anomalies, multilepton anomalies, the *X*17 excess, the di-di-jet excesses and the Higgs-like signals.

Competing interests

The authors declare no competing interests.

Additional information

Peer review information *Nature Reviews Physics* thanks Mitesh Patel, Mark Smith and the other, anonymous, reviewer(s) for their contribution to the peer review of this work.